

JRC TECHNICAL REPORTS



New sensors benchmark report on Kompsat-3

*Geometric benchmarking over
Maussanne test site for CAP
purposes*



Blanka Vajsova
Agnieszka Walczynska
Samuel Bärish
Pär Johan Åstrand
Susanne Hain

2014

Report EUR 27064 EN

European Commission
Joint Research Centre
Institute for Environment and Sustainability

Contact information

Pär Johan Åstrand

Address: Joint Research Centre, Via Enrico Fermi 2749, TP 263, 21027 Ispra (VA), Italy

E-mail: par-johan.astrand@jrc.ec.europa.eu

Tel.: +39 0332 78 6215

JRC Science Hub

<https://ec.europa.eu/jrc>

Legal Notice

This publication is a Technical Report by the Joint Research Centre, the European Commission's in-house science service.

It aims to provide evidence-based scientific support to the European policy-making process. The scientific output expressed does not imply a policy position of the European Commission. Neither the European Commission nor any person acting on behalf of the Commission is responsible for the use which might be made of this publication.

All images © European Union 2014, except: Figures 1-10 © European Space Imaging 2014

The geographic borders are purely a graphical representation and are only intended to be indicative. The boundaries do not necessarily reflect the official position of the European Commission.

JRC93093

EUR 27064

ISBN 978-92-79-45054-9

ISSN 1831-9424

doi:10.2788/240349

Luxembourg: Publications Office of the European Union, 2015

© European Union, 2015

Reproduction is authorised provided the source is acknowledged.

Abstract

The following document has been drawn up as a follow up to the Quality Control Record L [i] on the commissioning phase of the Kompsat-3 imagery, planned benchmarking tests as well as the methodology used in the tests. Benchmarking is necessary to be performed in order to estimate the usability of the imagery collected by particular sensor in The Common Agricultural Policy (CAP) image acquisition Campaign. The main requirement that should be fulfilled concerns the planimetric accuracy of the orthoimagery which should not exceed particular thresholds given in VHR Specifications [iii]. The methodologies used in the benchmarking tests were performed based on Guidelines for Best Practice and Quality Checking of Ortho Imagery [ii]. However, in addition the tests were performed according to alternative methodology, described in [i], which differs from the standard one, the GCPs selection/measurement phase i.e. image to image correlation techniques are used.

Table of contents:

List of Annexes:.....	ii
Abbreviations used in this report:	iii
Introduction.....	4
1. Kompsat-3 satellite	4
1.1 Satellite sensor characteristics - design.....	4
1.2 Satellite sensor characteristics – specifications	5
1.3 Kompsat-3 image data.....	5
2. Study area and Kompsat-3 data for testing.....	6
3. Auxiliary data	7
3.1 Ground Control Points	7
3.2 Digital Elevation Model.....	9
3.3 Aerial Orthomosaics	11
3.4 Software	11
4. Methodology.....	11
4.1 Standard benchmarking methodology according to Guidelines for Best Practice and Quality Checking of Ortho Imagery [xii], [xiii], [xiv], [xv], [xvi], [xvii], [xviii].	11
4.2 Alternative Benchmarking Method	13
4.3 Sensor Alignment Issue.....	17
4.4 Additional tests.....	18
5. Summary and Conclusions	19
References.....	24
Annex I - External Quality Control of Kompsat-3 orthoimagery report (by JRC)	

List of tables:

Table 1: Satellite sensor characteristics – design.....	4
Table 2: Satellite sensor characteristics - specifications.....	5
Table 3: Product Specification – Kompsat-3	5
Table 4: Basic metadata of the Kompsat-3 sample imagery	7
Table 5: Ground Control Points Specifications [ix], [x], [xi]	7
Table 6: Ground Control Points selected to be used for Kompsat-3 benchmarking.....	8
Table 7: Digital Elevation Model Specifications	9
Table 8: Aerial Orthomosaics Specifications	11
Table 9: Scenarios for benchmarking according to Standard methodology.....	13
Table 10: Scenarios for alternative benchmarking tests.....	16
Table 11: Additional tests performed	18
Table 12: Scenarios for additional tests in Intergraph Erdas 2013.....	18
Table 13: Scenarios for additional tests in PCI Geomatica OrthoEngine 2013.....	18
Table 14: Additional tests - 15deg ONA image	19
Table 15: Scenarios-in accordance to Guidelines for Best Practice and Quality Checking of Ortho Imagery.....	20
Table 16: Scenarios-in accordance to new alternative methodology	20
Table 17 - SUMMARY of RMSE.....	22

List of figures:

Figure 1: Location of the testing site	6
Figure 2: Spatial resolution as a function of 1). Elevation Angle, 2). Off nadir angle – Kompsat-3.....	9
Figure 3: ADS40_Ortho versus ADS40_PseudoDTM.....	10
Figure 4: ADS40_Ortho versus INTERMAP_5mDTM	10
Figure 5: Standard benchmarking procedure	12
Figure 6: Distribution of the GCPs over testing AOI.....	12
Figure 7: Image chip distribution-an example (size of the chip is superimposed for a better visualisation)	14
Figure 8: Example selections for the Reference Chip Database.....	15
Figure 9: Distribution of the GCPs (and the reference chips) over testing AOI	16
Figure 10: Sensor alignment calibration	17

List of Annexes:

Annex I: EXTERNAL QUALITY CONTROL OF KOMPSAT-3 ORTHOIMAGERY REPORT
Annex II: INTERNAL QUALITY CONTROL REPORTS
Annex III: EXTERNAL QUALITY CONTROL REPORTS

Abbreviations used in this report:

AD	Attitude Determination
ADS	Airborne Digital Sensor
AOI	Area of Interest
CAP	The Common Agricultural Policy
CE ₉₀	Circular Error of 90%
COTS	Commercial off-the-shelf
CPU	A central processing unit
DEM	Digital Elevation Model
DSM	Digital Surface Model
EO	Earth Observation
EPSG	European Petroleum Survey Group
EQC	External Quality Control
EUSI	European Space Imaging
FFT	Fast Fourier Transform
FFTP	Fast Fourier Transform Phase
GCP	Ground Control Point
GPS	The Global Positioning System
GSD	Ground Sample Distance
IPC	Independent Check Point
IQC	Internal Quality Control
JRC	Joint Research Centre
KARI	The Korea Aerospace Research Institute
LE ₉₀	Linear Error of 90%
LPIS	Land Parcel Information System
LVLH	Local Vertical/Local Horizontal
MS	Multispectral
MSL	Mean Sea Level
MTF	Modulation Transfer Function
NCC	Normalized Cross Correlation
NDVI	The Normalized Difference Vegetation Index
OD	Orbit Determination
ONA	Off Nadir Angle
PAD	Precision Attitude Determination
PAN	Panchromatic
POD	Precision Orbit Determination
RMSE	Root Mean Square Error
RPC	Rational Polynomial Coefficient
SAR	Synthetic-Aperture Radar
SI	Satrec Initiative
TP	Tie Point
UTM	Universal Transverse Mercator
VHR	Very High Resolution
WGS 84	World Geodetic System 1984
1-D	One-dimensional

Introduction

The requirement for the planimetric accuracy of the orthorectified Very High Resolution Satellite Imagery used with scope of the Control with Remote Sensing Programme according to the “Guidelines for Best Practice and Quality Checking of Ortho Imagery” [ii] is as follows: the two dimensional RMSE (Root Mean Square Error) measured on Independent Check Points (ICPs) and calculated individually for Northing and Easting direction must not exceed 2m for VHR Prime and 5m for VHR Backup [i,vi]. Therefore, two Kompsat-3 satellite images have been assessed to assign the sensor to VHR Prime or Backup profile.

The benchmarking tests have been performed according to Guidelines for Best Practice and Quality Checking of Ortho Imagery [ii] as well as according to alternative benchmarking methodology described in [j] and accepted by JRC. The produced orthoimages have been delivered to JRC for the further analysis i.e. external quality control. The external quality control outcome will allow to:

- estimate the usability of the imagery for the CAP (The Common Agricultural Policy) checks i.e. to evaluate the planimetric accuracy (1D RMSE calculated on Independent Check Points - ICPs) should not exceed: 2m for VHR Prime Profile, 5m for VHR Backup)
- measure the influence of the different factors, e.g. number of GCPs, incidence angle, sensor model on the geometric accuracy of the orthoimagery
- evaluate the planimetric accuracy that can be reached using 2 different softwares: PCI Geomatica and Intergraph ERDAS Imagine as well as sensor model implemented within tested software.

1. Kompsat-3 satellite

Launched in May 2012, KOMPSAT-3 is a Korean remote sensing satellite, operated by The Korea Aerospace Research Institute (KARI) in cooperation with Satrec Initiative (SI), which provides 0.7 m GSD panchromatic image and 2.8 m GSD multi-spectral image data. The Mission orbit of the KOMPSAT-3 is a sun-synchronous near-circular orbit with an altitude of 685.12 km. The orbit inclination is 98.13 degrees and the satellite operates (in contrast to most other optical VHR satellites) with a nominal local time of ascending nodes of 13:30 PM. KOMPSAT-3 provides the highest bit per pixels (14 bits/pixel) among commercial satellites. Additionally, due to its enhanced radiometric depth, more detailed classification results can be acquired [iv, v].

1.1 Satellite sensor characteristics - design

Launch information	Date: 18.05.2012 Launch Vehicle: H-IIA launch system Launch Location: Tanegashima Space Center of JAXA, Japan
Satellite weight/size/power	approx. 980 kg; 3.5 m height, 2.0 m diameter; 1.3 kW
Orbit	Altitude: 685 km Type: sun-synchronous near-circular Period: 98.58 min
Inclination/Equator Crossing Time	98.13 deg/ 13:30pm (ascending node)
Orbits per day	409R28D : 409 orbits per 28 days. 14.6 orbits per day
Revisit rate	3.5 days average revisit time at +/- 30 deg tilt angle over equator area

Table 1: Satellite sensor characteristics – design

1.2 Satellite sensor characteristics – specifications

Sensor bands (spectral range)	Pan & 4 MS: Panchromatic: 450 – 900 Blue: 450 – 520 Green: 520 – 600 Red: 630 – 690 NIR: 760 – 900
Sensor Resolution (at nadir)	0.70 m panchromatic 2.80 m multispectral
Dynamic Range	14 bits/pixel
Swath Widths	16 km at nadir
Geolocation Accuracy (CE90)	< 48.5 meter (CE90) : measured < 70 meter (CE90) : system specification
Capacity	Global: 300,000 km ² per day 109,500,000 km ² per year KOMPSAT-3 can be tilted up to +/-56 degree from LVLH about roll axis (nominal operation range is +/-30 degree) and up to +/-30 degree about pitch axis Imaging Modes: Strip Imaging Multi Point Imaging Single Pass Stereo Imaging Wide Area Along Imaging
Expected End of Operational Life	Expected life time > 7 years

Table 2: Satellite sensor characteristics - specifications

1.3 Kompsat-3 image data

The standard processing level of Kompsat-3 imagery that is provided to the users is Level 1R (Basic/Option) or Level 1G. Table 3 shows specifications for the Products: Level 1R and Level 1G.

Product level	1R (Basic)	1R (Option)	1G (Standard)
Horizontal Accuracy* (m, CE90) Specification (Expectation) *excluding terrain effect	285,0	70,0 (50,0)	70,0 (50,0)
Maximum off-nadir angle (degree)	30	30	30
Nominal GSD at nadir (m)	0,7	0,7	0,7
Products/band combination	bundle (pan + 4 multispectral) pan-sharpened (4 pan-sharpened bands).	bundle (pan + 4 multispectral) pan-sharpened (4 pan-sharpened bands).	bundle (pan + 4 multispectral) pan-sharpened (4 pan-sharpened bands).
Processing:	-without GCP -using OD/AD -Radiometric correction -sensor correction -MTF compensation -Geo-information included	-without GCP -using POD/PAD -Radiometric correction -sensor correction -MTF compensation -Geo-information included	-without GCP -using POD/PAD -Radiometric correction -sensor correction -MTF compensation -Geometrical correction

Table 3: Product Specification – Kompsat-3

2. Study area and Kompsat-3 data for testing

Testing AOI shown in Figure 1 is located in French commune Maussane-les-Alpilles in the Provence-Alpes-Cote d'Azur region in southern France. The AOI in France had been used as a test site by the European Commission since 1997 and is characterized by different land use types and the terrain variations (high difference between highest and lowest point is around 300m). The area used in the tests is 100km² and spans 4° 41' to 4° 48'E and 43° 40' to 43° 45'N.

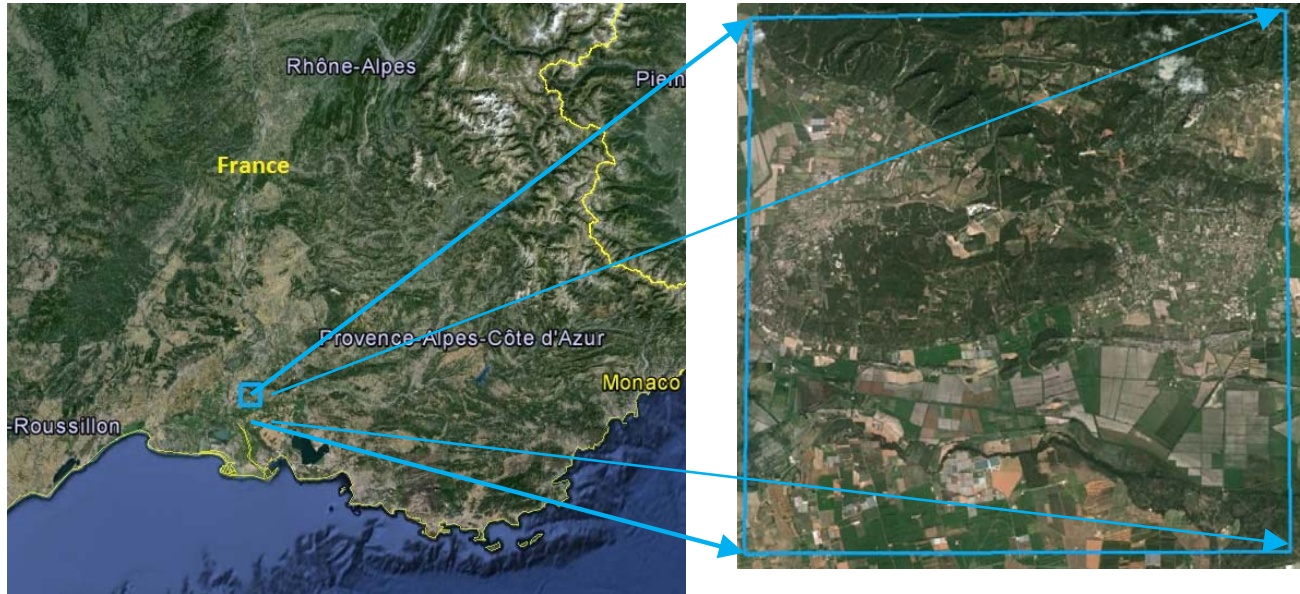


Figure 1: Location of the testing site

Samples of the Kompsat-3 imagery used for testing were collected in November and December 2013 at two different elevation angles: low and high. Basic metadata are shown in Table 4.

Image id (internal image id)	K3_20131201124325_08224_01071327_L1R	K3_20140922124354_12533_01071327_L1R	K3_20131129130507_08195_01071327_L1R
Image short ID	K3_1	K3_2	K3_3
Product level	Level1R (Option)	Level1R (Option)	Level1R (Option)
Product Type	Pan Sharpened	Pan Sharpened	Pan Sharpened
Collection date	01.12.2013	22.09.2014	29.11.2013
Azimuth (Azimuth angle when the center pixel of the image has been acquired)	258.64deg	260.04	262.50deg
Roll Tilt Angle (rotation about the in-track direction)	-0.97deg	-11.63deg	-32.27deg
Across-Track Angle			
Pitch Tilt Angle (rotation about the in-track direction)	-0.175deg	-0.165deg	-0.14deg
In-Track Angle			
Yaw Tilt Angle	-2.75deg	-2.73deg	-2.32deg
Incidence Angle	1.12deg	12.97deg	36.28
SunAngle:			
-Azimuth	200.61deg	266.97deg	201.13deg
-Elevation	27.42deg	45.23deg	28.18deg

Off nadir angle	1deg	11.63deg	32deg
Elevation Angle	89deg	77deg	54deg
Ellipsoid Type/ Projection	WGS-84/UTM, N31		
Format	GeoTIFF		
RPC files	yes		
Bits Per Pixel	14		
Resampling Method	4x4cubic convolution		

Table 4: Basic metadata of the Kompsat-3 sample imagery

3. Auxiliary data

The following auxiliary data are necessary in order to perform the orthorectification:

- Ground Control Points
- Digital Elevation Model
- Aerial Orthomosaics (applicable for 4.2)

3.1 Ground Control Points

Ground Control Points are usually used to orthorectify the satellite imagery and are necessary to control the orthoimagery accuracy. According to the "Guidelines for Best Practice and Quality Checking of Ortho Imagery" [ii] the accuracy of the GCPs used in the orthorectification should be at least 3 times (5 times recommended) more precise than the target specification for ortho.

Target specification for ortho [iii] is as follows:

- VHR prime: 1-DRMSE error measured separately for X and Y should not exceed 2m
- VHR backup: 1-DRMSE error measured separately for X and Y should not exceed 5m.

For the testing AOI (see chapter 2) there is a set of GCPs available to perform the benchmarking. GCPs (Table 5) were collected by JRC and have been provided to EUSI for the Kompsat-3 benchmarking tests:

Dataset	Point ID	RMSE x [m]	RMSEy [m]	Projecti on and datum	Source
ADS40 GCP_dataset_Maussane_prepared_for_ADS 40_in_2003	11XXXX	0,05	0,10	UTM 31N WGS84	GPS measurem ents
VEXCEL_GCP_dataset_Maussane_ prepared_for_VEXEL_in_2005	44XXX	0,49	0,50		
Multi-use_GCP_dataset_Maussane_ prepared_for_multi-use_in_Oct-2009	66XXX	0,30	0,30		
Cartosat- 1_GCP_dataset_Maussane_prepared_ for_Cartosat_in_2006	33XXX	0,55	0,37		
Formosat-2_GCP_dataset_Maussane_ prepared_for_Formosat2_in_2007	7XXX	0,88	0,72		
Cartosat-2_GCP_dataset_Maussane_ prepared_for_Cartosat-2_in_2009	55XXX	0,90	0,76		
SPOT_GCP_dataset_Maussane_ prepared_for_SPOT_in_	22XXX	n/a	n/a		

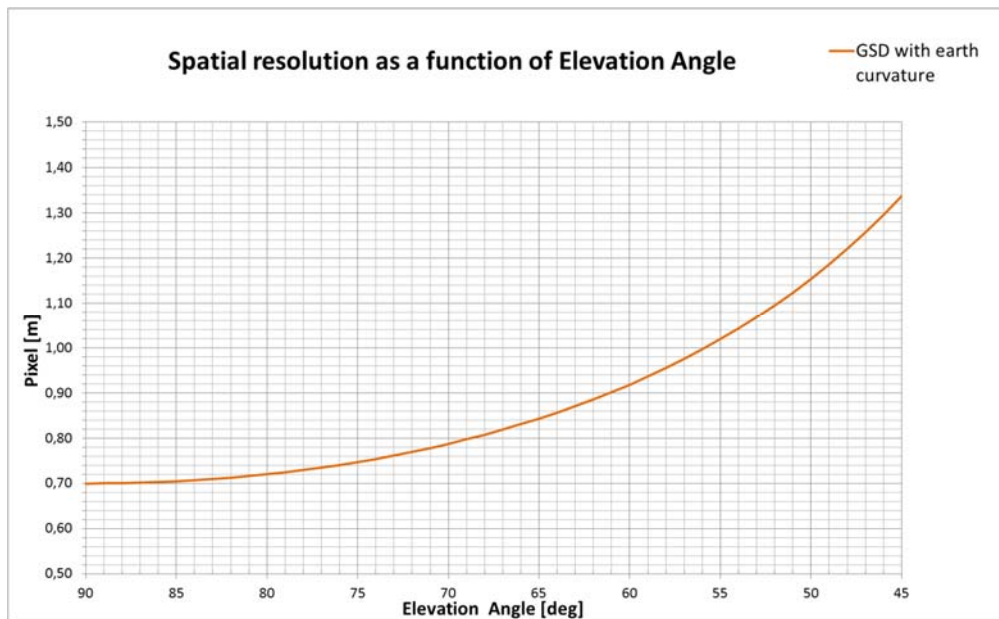
Table 5: Ground Control Points Specifications [ix], [x], [xi]

12 well distributed GCPs, used during the geometric correction model phase, were selected as a subset from the dataset described in Table 5, i.e.:

#	ID	GCP ₃	GCP ₄	GCP ₆	GCP ₉	GCP ₁₂
1	66003	x	x	x	x	x
2	66007				x	x
3	66021	x	x	x	x	x
4	66022					x
5	66025				x	x
6	66029				x	x
7	66035		x	x	x	x
8	66039			x	x	x
9	110016					x
10	440005	x	x	x	x	x
11	440009					x
12	440015			x	x	x

Table 6: Ground Control Points selected to be used for Kompsat-3 benchmarking

1).



2).

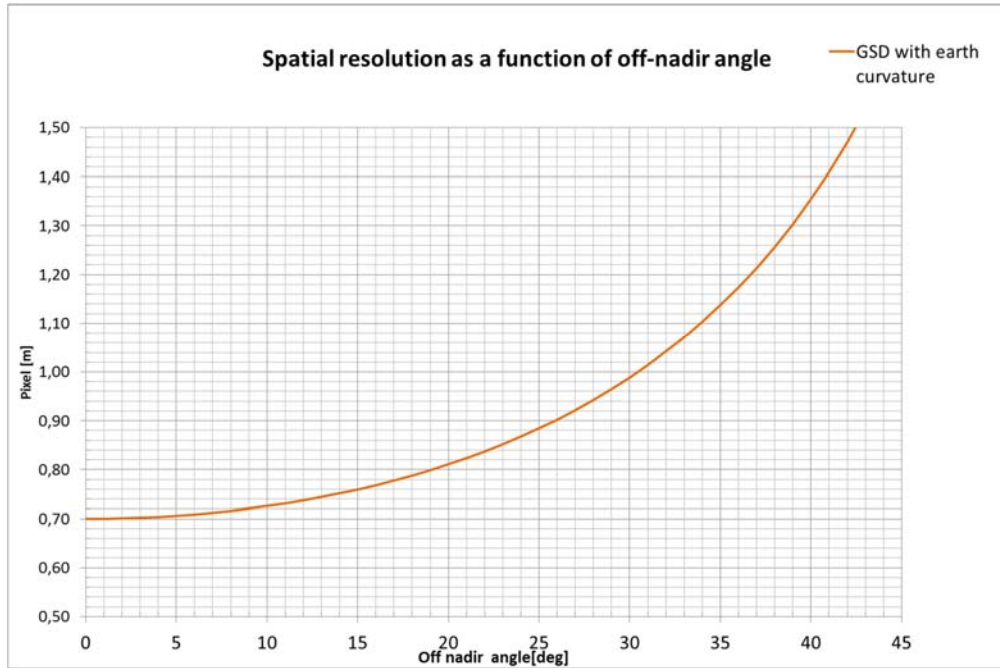


Figure 2: Spatial resolution as a function of 1). Elevation Angle, 2). Off nadir angle – Kompsat-3

3.2 Digital Elevation Model

To perform the orthorectification i.e. to accurately remove the distortions from the image (that comes from the sensor and the earth's terrain) a Digital Elevation Model is used. Several factors play an important role concerning the quality of the DEM e.g. grid size and the vertical accuracy. Table 7 contains the specification of the DEMs that were used for Kompsat-3 benchmarking tests.

Data set	Grid size	Accuracy	Projection and datum	Source
DEM_ADS40	2m x 2m	RMSEz ≤ 0,60m	UTM 31N WGS84 (EPSG 32631)	ADS40 (Leica Geosystems) digital airborne image of GSD 50cm
INTERMAP5mDTM	5m x 5m	1m RMSE for unobstructed flat ground		aerial SAR

Table 7: Digital Elevation Model Specifications

Although the specification of DEM_ADS40 is much better than INTERMAP5mDTM, the majority of the tests were performed using the Intermap DTM. DEM_ADS40 has been edited/filtered for agriculture areas (but the delineation of these areas seems to be very rough, Figure 3/Figure 4) therefore some areas e.g. forest areas could suffer from smearing effects in the orthoimagery performed on K3_3 image for which the elevation angle is 54deg. The INTERMAP5mDTM seems to be a good compromise (although some steep areas also suffer from smearing). Nevertheless, a comparison of height values in open areas (where most of the GCPs are situated) show only minor differences between the two DTMs.

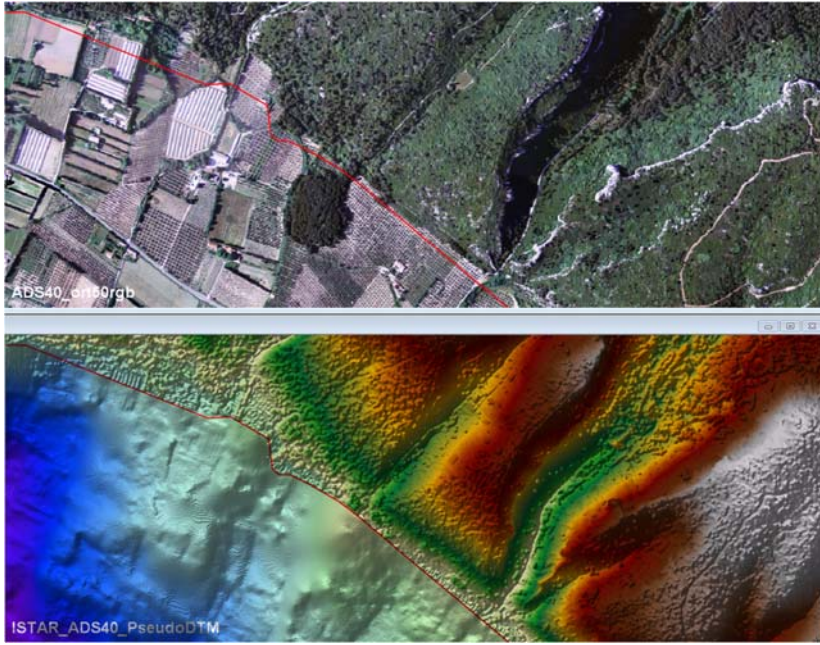


Figure 3: ADS40_Ortho versus ADS40_PseudoDTM

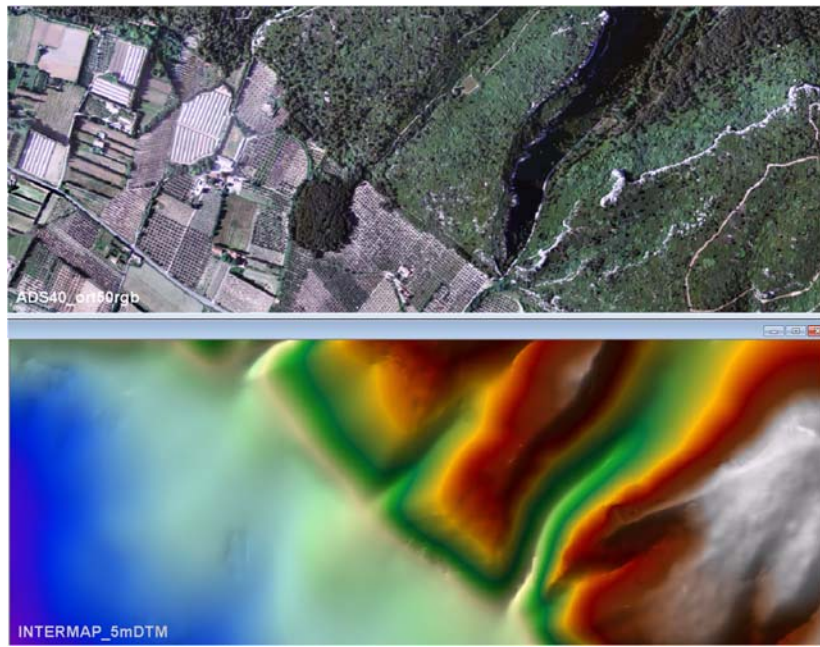


Figure 4: ADS40_Ortho versus INTERMAP_5mDTM

3.3 Aerial Orthomosaics

An Aerial Orthomosaics acquired by ADS40 for which the grid size is 0,5m has been used as a raster reference in the Alternative Benchmarking Method. The specification is given in Table 8.

Aerial Orthomosaics	Grid size	Accuracy	Projection datum and	Source
ADS40	0,5m	n/a	UTM 31N WGS84	ADS40 aerial flight by ISTAR, 2003. Bands: R, G, B, IR, PAN

Table 8: Aerial Orthomosaics Specifications

3.4 Software

Currently, the orthorectification module for Kompsat-3, Level 1R is implemented into the following software which is available to the contractor:

- PCI Geomatica 2013 (Rigorous and Rational Function Model) [vii]
- Intergraph ERDAS Imagine 2013 (Rational Function Model) [viii]

4. Methodology

Benchmarking tests were performed according to the procedure described in Guidelines for Best Practice and Quality Checking of Ortho Imagery [ii] as well as a new alternative methodology proposed by EUSI in Quality Control Record L on Kompsat-3 imagery [i].

In both cases, the main aim was to estimate the usability of the imagery for the CAP (The Common Agricultural Policy) checks i.e. to evaluate the planimetric accuracy (1D RMSE calculated on Independent Check Points - ICPs) that should not exceed: 2m for VHR Prime Profile, 5m for VHR Backup.

In the described tests 2 single scenes of Kompsat-3 imagery (see chapter 2) were orthorectified but different factors were considered by varying the number of GCPs, the elevation angle, the algorithms used in image correction phase and the COTS in order to check their influence on the planimetric accuracy.

4.1 Standard benchmarking methodology according to Guidelines for Best Practice and Quality Checking of Ortho Imagery [xii], [xiii], [xiv], [xv], [xvi], [xvii], [xviii].

The following phases describe the sequence of steps needed to carry out the benchmarking tests of the Kompsat-3 imagery in accordance with the Guidelines for Best Practice and Quality Checking of Ortho Imagery (Figure 5):

Phase 1: Modelling - geometric correction model phase, also referred as to image correction phase, sensor orientation phase, space resection or bundle adjustment phase. Sensor models are mathematical models that define the physical relationship between image coordinates and ground coordinates, and they are different for each sensor. In this phase Ground Control Points are used for improving absolute accuracy. Figure 6 shows visual distribution and configuration of the GCPs (which are also listed in chapter 3.1). However, the tests were also performed without using GCPs in this phase - please see Figure 5 with the scenarios performed.

Phase 2: Orthorectification - the phase where distortions in image geometry caused by the combined effect of terrain elevation variations and non-vertical angles from the satellite to each point in the image at the time of acquisition are corrected.

Phase 3: External Quality Control (EQC) of the final product - described by 1-D RMSE_x and 1-D RMSE_y – performed by JRC. According to Guidelines for Best Practice and Quality Checking of Ortho Imagery [ii] minimum 20 check points should be checked in order to assess orthoimage planimetric accuracy. The points used during the geometric correction phase should be excluded.

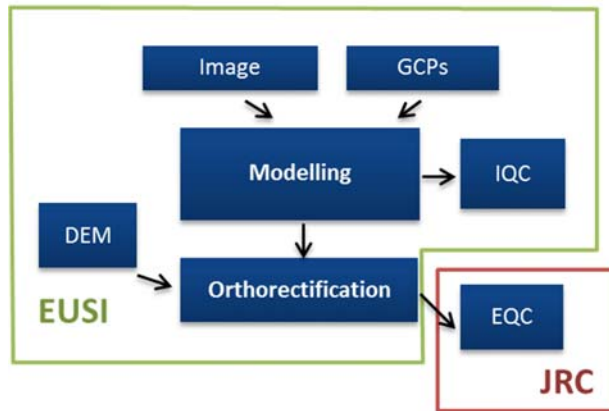


Figure 5: Standard benchmarking procedure

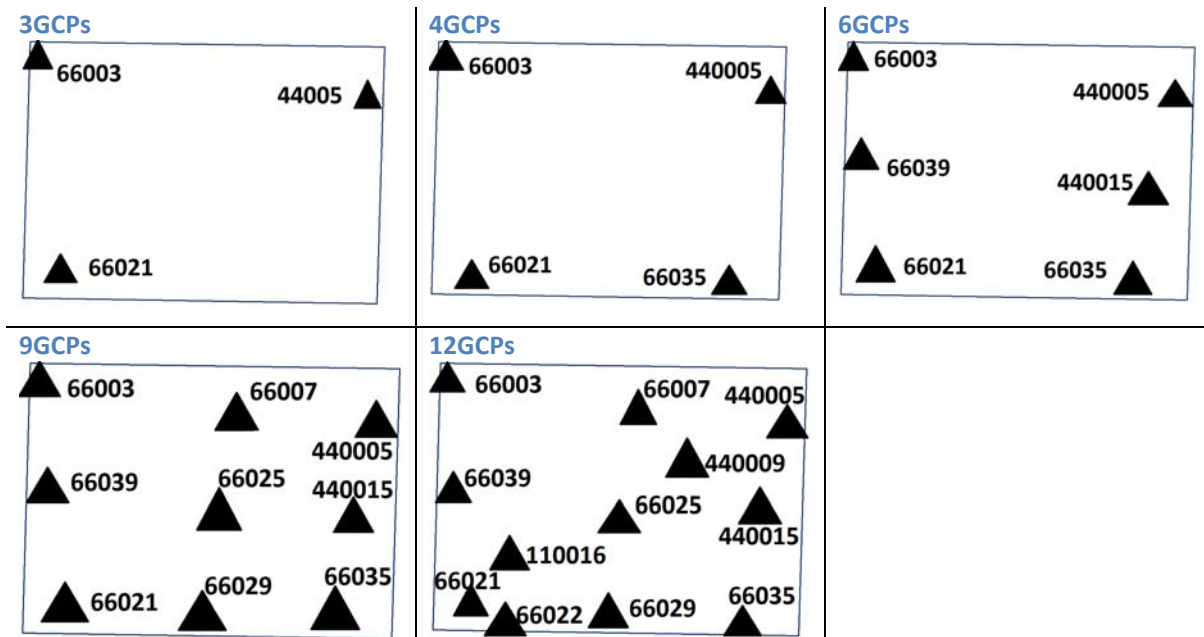


Figure 6: Distribution of the GCPs over testing AOI

To summarize, 26 orthoimagery have been performed based on auxiliary data described in chapter 3.1, 3.2 and 2. For the orthorectification of the Kompsat-3 imagery 2 COTS were used and 2 sensor models implemented into the softwares – all scenarios are shown in Table 9. RPCo polynomial model is implemented in both COTS that have been used - this allows comparison of two algorithms/softwares. Nonetheless, the Rigorous model is only implemented in PCI Geomatics 2013, not available in Intergraph Erdas 2013.

COTS	Sensor Model – Phase 1	Number of GCPs - Phase 1	DEM	Number of Images	Number of orthoimagery
PCI Geomatics 2013	RPC o polynomial	0	INTERMAP ₅ mDTM/ DSM ADS ₄₀ *	2	2
		3			2
		4			4
		6			2
	Toutins Rigorous	6			2
		9			2
		12			2
Intergraph Erdas 2013	RPC o polynomial	0	INTERMAP ₅ mDTM/ DSM ADS ₄₀ *	2	2
		3			2
		4			2
		6			2
*DSM ADS ₄₀ used only for 4GCPs, RPCo in PCI Geomatics 2013 and Intergraph Erdas 2013					<i>In total 26 orthos</i>

Table 9: Scenarios for benchmarking according to Standard methodology

4.2 Alternative Benchmarking Method

The alternative procedure for performing benchmarking tests is based on the standard procedure i.e. the following steps are performed: Modelling, Orthorectification, External Quality Control (EQC) of the final product. In the standard procedure (chapter 4.1) the Ground Control Points used in the Modelling Phase are selected manually from the existing data set (chapter 3.1).

It can be concluded from several publications like the following [xix], [xx] and was mentioned in the report of a previous sensor benchmark carried out by Joint Research Centre (JRC) [xvi], [xvii] that the manual selection of ground control points is often limited by sufficient accuracy and repeatability (e.g. different operators). Also, it happens often, that the auxiliary data (GCPs) collected few years ago, due to the land use and land cover change cannot be identified in the new collected image that is supposed to be orthorectified.

As an alternative method for performing benchmarking tests we proposed in [i] the automatic selection of the Ground Control Points using an image registration function also called image-to-image correlation techniques. It has been proven that image-to-image correlation techniques are a valuable instrument in satellite image processing and are going to play a more important role in the future [xxiii],[xxiv]. In image-to-image correlation techniques 2 images are needed: a raster reference image and the target image (image to be mapped onto the reference image).

Existing automated registration techniques can be divided into the following classes [xxi]:

- area based methods (i.e. normalized cross correlation method or fast Fourier transform-based (FFT-based))
- feature based methods (attempt to find the correspondence and transformation using distinct anatomical features that are extracted from images based on lines, curves, points, line intersections, boundaries, etc.).

Several satellite image processing SW packages are providing now extended tools and functions for automatic retrieval of Tie Points (TPs) and Ground Control Point (GCPs). PCI Geomatica OrthoEngine 2013 provides an "Automatic GCP collection" module which has two options for the matching process: NCC (Normalized Cross Correlation) and FFTP (Fast Fourier Transform Phase).

Also extended tools and functions for automatic retrieval of Tie Points (TPs) and Ground Control Point (GCPs) are included in many satellite image processing environments. PCI Geomatica OrthoEngine 2013 e.g. provides an "Automatic GCP collection" module which again has two options

for the matching process: NCC (Normalized Cross Correlation) and FFTP (Fast Fourier Transform Phase).

PCI recommends using the FFTP option for consistent matching of the results especially between images from different sensors or with different grey value distribution: "For more consistently accurate results, FFTP is recommended. This method uses a larger template size than NCC and, because it works in the frequency domain, it looks at the patterns of details in the image rather than the grey values in a small neighbourhood, which NCC uses. This makes FFTP more robust than NCC in cases where there is a large brightness difference between images or when a major land use change has occurred between the images and allows it to better match images of the same area from different sensors or spectral bands" [vii].

A good comparison of different image matching techniques regarding the registration of satellite imagery can be found in [xxv].

The proposed Fast Fourier Template matching has also proven to be a valuable technique within other European earth observation contexts like emergency mapping. See [xxi].

Although automatic image matching techniques are well suited to define very accurate relations between different raster datasets, the problem with extracting a correct height value from an additionally available height source (DTM or DSM) occurs. Such problems arise mainly in areas where buildings or high vegetation are not modelled correctly by the elevation model and/or where horizontal displacements of such features caused by different azimuth and elevation lead to wrong values for corresponding points in the matched images. Additionally most DEMs suffer from slightly worse vertical accuracies in areas with high slope angles. That is why the automatic GCP collection process should be guided through sub-selecting areas from the reference image where the above mentioned limitations could be avoided:

- A slope map will be calculated for the DEM used and a threshold for a maximum slope value will be defined
- A point database will be established based upon the reference image and the calculated height map for marking the centre of image subsets where slope and surface dependent inaccuracies could be avoided
- This point database will then serve as basis for extracting an image chip database out of the reference imagery
- Finally the chip database is used to automatically extract reference points by use of image matching techniques (preserving a good distribution of the control point of the GCPs in the image).

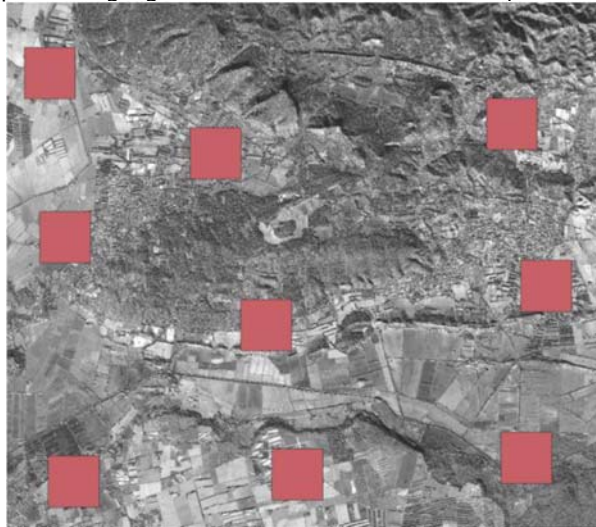


Figure 7: Image chip distribution-an example (size of the chip is superimposed for a better visualisation)

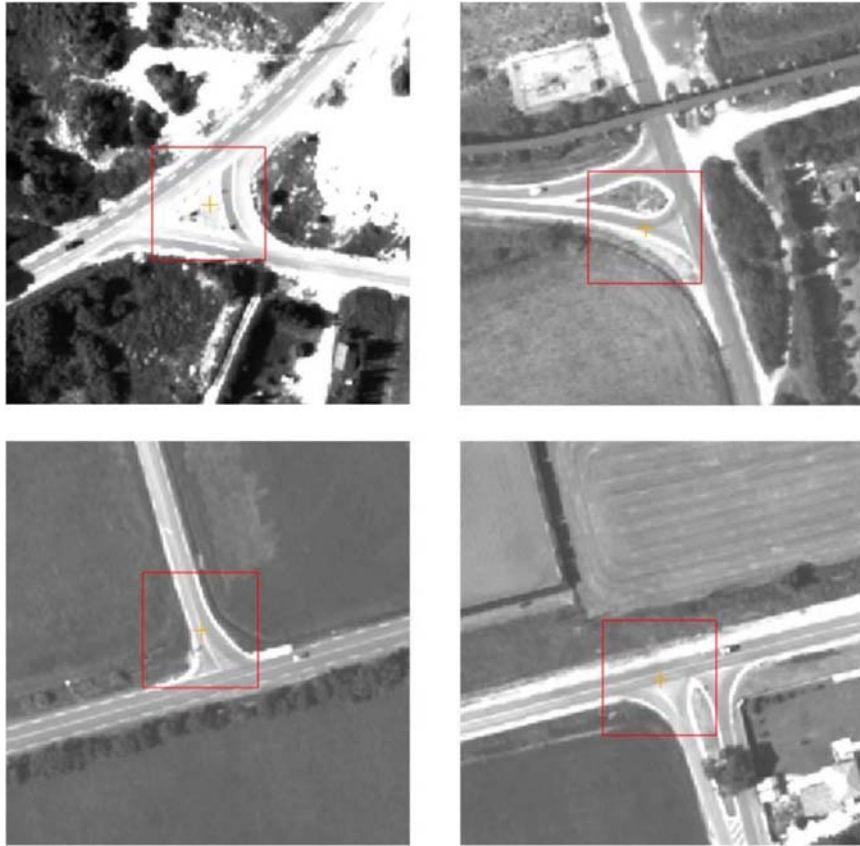


Figure 8: Example selections for the Reference Chip Database

In the performed, alternative tests a chip database was prepared i.e. small subsetting images extracted from the ADS40 orthomosaic were collected and ADS40 orthomosaics acted as a raster reference while Komsat-3, level 1R image (first K3_1 and then K3_3) was the target image. Each chip has a GCP number associated with it, which corresponds to GCP selected from the batch provided by JRC (Table 5) i.e. the centre of the chip is exactly at the location of the GCP (Table 6 and Figure 9). This allows for a good comparison between: manually adapting GCP coordinates and image to image registration function (however, operator could go for a different chip positions which would also serve a good correlation reference).

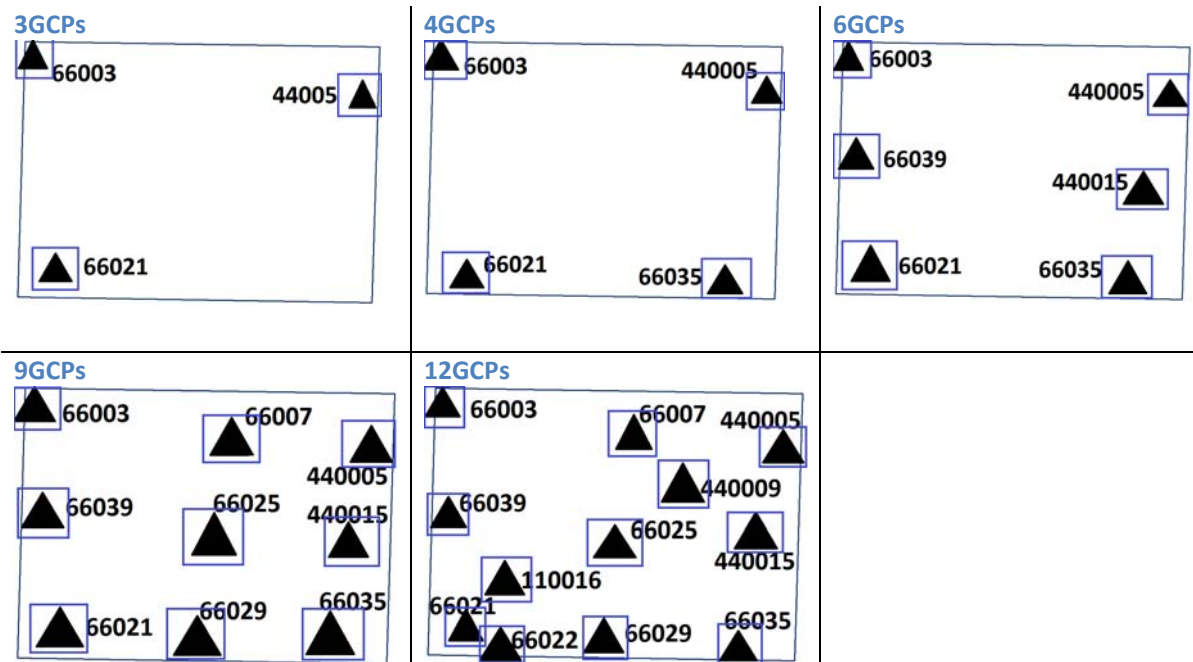


Figure 9: Distribution of the GCPs (and the reference chips) over testing AOI

COTS	Sensor Model - Phase 1	Number of GCPs - Phase 1	DEM	Number of Images	Number of orthoimagery
PCI Geomatica OrthoEngine 2013	Toutin's Rigorous Model	6GCPs	INTERMAP _{5m} DTM/ DSM ADS ₄₀ *	2	2
		9 GCPs			2
		12GCPs			2
	Rational Function Model (0 order polynomial)	3GCPs			2
		4GCPs			4
		6GCPs			2
*DSM ADS ₄₀ used only for 4GCPs, RPCo in PCI Geomatics 2013 and Intergraph Erdas 2013					In total 14 orthos

Table 10: Scenarios for alternative benchmarking tests

To summarize, 14 orthoimagery have been produced based on auxiliary data described in chapter 3.1, 3.2, 3.3 and 2. For the orthorectification of the Kompsat-3 imagery PCI Geomatica OrthoEngine 2013 was used and 2 sensor models implemented into software – all scenarios are shown in Table 10. The image-to-image registration function is not yet available in Intergraph Erdas 2013. However, the performed scenarios allow to compare the new methodology with the standard one.

4.3 Sensor Alignment Issue

Each sensor is being checked on a regular basis whether data received from the satellite meets system specifications (or whether re-calibration and alignment should be performed). Among others, geometric mapping performance such as location accuracy is being determined. After evaluation of in-orbit geolocation by satellite provider, it turned out that there is a strong bias error in the east direction. Therefore, sensor alignment, re-calibration in cross-track direction, was required to be performed (Figure 10, provided by KARI). This problem, related to east direction, is expected to be solved (by updating processing software) in October 2014.

- **Location Accuracy**

- KOMPSAT-3 Sensor alignment calibration

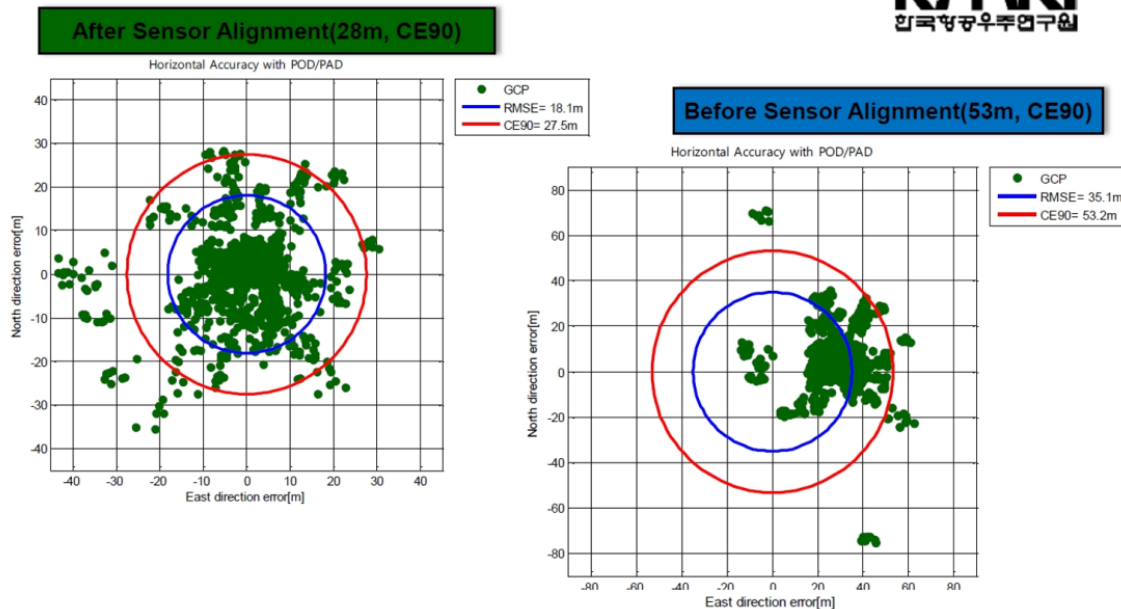


Figure 10: Sensor alignment calibration

The bias in east direction has not yet been taken into account in PCI Geomatica OrthoEngine 2013 algorithms. The assumption is that the errors are distributed normally and the software does not expect the errors to be biased in one direction. Thus, the standard accuracy values for GCPs in the modelling phase have influence on modelling phase as well as the accuracy of created ortho. Therefore, our first tests performed in PCI Geomatica OrthoEngine 2013 (Rational Function Model, 0 order polynomial, chapter 4.2 and o) suffer from a bias in east direction which has been discovered after our careful analysis of created orthos.

The problem can be solved by changing standard accuracy parameters for GCPs and thus by giving more weight to the reference coordinates (from 1.0m in X, Y, Z to 0.000001m in X, Y and 0.0001m in Z). PCI solved this issue in the 2014 Release of Geomatica which could be verified by comparing orthoimagery created in PCI Geomatica OrthoEngine 2013 (using alternative weighting parameters) to orthoimagery created in PCI Geomatica OrthoEngine 2014 (using standard parameters). Also the comparison with orthoimagery created in ERDAS for each of the respective test scenarios that have been carried out, showed a better consistence when adapted parameters were used. The following orthoimagery (in total 16) have been re-delivered for the EQC:

COTS	Sensor Model Phase 1	Number of GCPs - Phase 1	DEM	Methodology	Nr. of Images	Nr. of orthoimagery
PCI Geomatics 2013	RPC o polynomial	3 GCPs	INTERMAP5mDTM/ DSM ADS40*	- in accordance with Guidelines for Best Practice and Quality Checking of Ortho Imagery (4.1) -in accordance to new alternative methodology (4.2)	2	4
		4 GCPs				8
		6 GCPs				4
*DSM ADS40 used only for 4GCPs						In total 16 orthos

Table 11: Additional tests performed

Due to the fact that Rigorous model does not take into account supplied RPC parameters and is sensitive to the accuracy of the GCPs, the sensor alignment issue has no impact on the ortho imagery created using Toutin's model and the standard accuracy parameters for accuracy of the GCPs can be considered.

4.4 Additional tests

Additional tests have been performed according to the standard methodology described in chapter 4.1 as per JRC request. Two orthoimagery have been created from image K3_1 (ONA 1deg), RPCo using 1GCP and 2GCPs. Similar scenario has been considered for the second image K3_3 (ONA 32deg), however in this case 9GCPs and 12GCPs were used in modelling phase-see Table 12.

COTS	Sensor Model – Phase 1	Number of GCPs - Phase 1	DEM	Number of Images	Number of orthoimagery
Intergraph Erdas 2013	Rational Function Model (o order polynomial)	1GCPs	INTERMAP5mDTM	1 (K3_1)	1
		2 GCPs			1
		9GCPs		1 (K3_3)	1
		12 GCPs			1
					In total 4 orthos

Table 12: Scenarios for additional tests in Intergraph Erdas 2013

To be able to compare sensor models implemented into two different COTS the same set of orthoimagery in PCI Geomatica OrthoEngine 2013 have been created.

COTS	Sensor Model – Phase 1	Number of GCPs - Phase 1	DEM	Number of Images	Number of orthoimagery
PCI Geomatica OrthoEngine 2013	Rational Function Model (o order polynomial)	1GCPs	INTERMAP5mDTM	1 (K3_1)	1
		2 GCPs			1
		9GCPs		1 (K3_3)	1
		12 GCPs			1
					In total 4 orthos

Table 13: Scenarios for additional tests in PCI Geomatica OrthoEngine 2013

In total 8 orthoimagery were delivered to JRC for performing EQC.

As per JRC request the tests will be performed additionally on an image collected at ONA ~15deg (once acquired, possible ONA range 12-17deg). According to the methodology given in chapter 4.1. The following scenario has been approved by JRC (EUSI/GAF performed in addition tests with oGCP):

COTS	Sensor Model – Phase 1	Number of GCPs – Phase 1	DEM	Number of Images	Number of orthos
Intergraph Erdas 2013	Rational Function Model (0 order polynomial)	0 GCP	INTERMAP5mDTM	1 (ONA 12-17deg)	3
		3 GCPs			
		4 GCPs			
PCI Geomatica OrthoEngine 2013	Rational Function Model (0 order polynomial)	0 GCP	INTERMAP5mDTM	1 (ONA 12-17deg)	3
		3 GCPs			
		4 GCPs			
	Toutin's Rigorous Model	6 GCPs	INTERMAP5mDTM	1 (ONA 12-17deg)	3
		9 GCPs			
		12 GCPs			
					<i>In total 9 orthos</i>

Table 14: Additional tests - 15deg ONA image

5. Summary and Conclusions

The benchmarking tests on Kompsat-3 satellite imagery have been performed in accordance with the Guidelines for Best Practice and Quality Checking of Ortho Imagery as well as in accordance to the new alternative methodology for the benchmarking tests which makes use of image registration techniques. Consequently, the usability of the Kompsat-3 imagery for The Common Agricultural Policy (CAP) checks can be estimated during the external quality control (Annex 1) performed by JRC i.e. checking whether the 1D RMSE (Root Mean Square Error: 1D RMSE_x, 1D RMSE_y) calculated on ICPs (Independent Check Points) does not exceed the thresholds of 2m and 5m respectively for VHR Prime and VHR Backup. The proposed in [i] new methodology can be compared with the standard one and the usability of the new method can be estimated. Also, the comparison between the two DTMs (less accurate INTERMAP5mDTM and more accurate DSM ADS40), 2 different COTS (ERDAS Imagine and PCI Geomatica) can be done. The sensitivity of Kompsat-3 orthoimage horizontal accuracy with respect to the satellite incidence angles, number and distribution of the GCPs used during the sensor orientation phase can be analysed. In total 64 orthoimagery have been produced and delivered to JRC for EQC (Annex 1), i.e.

- 42 according to 4.1:
 - Initially requested orthoimagery – 26 (Table 9)
 - Reprocessing due to alignment issue – 8 (Table 11)
 - Additionally requested by JRC tests – 8 (Table 12, Table 13)
- 22 according to 4.2
 - Initially requested orthoimagery – 14 (Table 10)
 - Reprocessing due to alignment issue – 8 (Table 11)

COTS	Sensor Model – Phase 1	Number of GCPs - Phase 1	DEM	Number of source imagery	Number of Orthoimagery produced
PCI Geomatica OrthoEngine 2013	Rational Function Model (0 order polynomial)	0	INTERMAP5mDTM	3	3
		1	INTERMAP5mDTM	1	1
		2	INTERMAP5mDTM	1	1
		3	INTERMAP5mDTM	2	2
		4	INTERMAP5mDTM/DSMADS40	2	8
		6	INTERMAP5mDTM	2	4
		9	INTERMAP5mDTM	1	1
	12	INTERMAP5mDTM	1	1	
	Toutin's Rigorous Model	6	INTERMAP5mDTM	2	2
		9	INTERMAP5mDTM	2	2
12		INTERMAP5mDTM	2	2	
Intergraph Erdas 2013	Rational Function Model (0 order polynomial)	0	INTERMAP5mDTM	3	3
		1	INTERMAP5mDTM	1	1
		2	INTERMAP5mDTM	1	1
		3	INTERMAP5mDTM	2	2
		4	INTERMAP5mDTM/DSMADS40	2	4
		6	INTERMAP5mDTM	2	2
		9	INTERMAP5mDTM	1	1
		12	INTERMAP5mDTM	1	1
<i>In total delivered to JRC</i>					44
<i>Excl. ortho imagery before taking into account sensor alignment issue</i>					36

Table 15: Scenarios-in accordance to Guidelines for Best Practice and Quality Checking of Ortho Imagery

COTS	Sensor Model – Phase 1	Number of GCPs - Phase 1	DEM	Number of source imagery	Number of Orthoimagery produced
PCI Geomatica OrthoEngine 2013	Rational Function Model (0 order polynomial)	3	INTERMAP5mDTM	2	4
		4	INTERMAP5mDTM/DSMADS40	2	8
		6	INTERMAP5mDTM	2	4
	Toutins Rigorous	6	INTERMAP5mDTM	2	2
		9	INTERMAP5mDTM	2	2
		12	INTERMAP5mDTM	2	2
<i>In total delivered to JRC</i>					22
<i>Excl. ortho imagery before taking into account sensor alignment issue</i>					14

Table 16: Scenarios-in accordance to new alternative methodology

Table 17 summarizes the test results. For the reports from modelling phase please see ANNEX II.

Off-nadir angle	Number of GCPs	Direction	RPC		Rigorous		DEM		
			PCI		PCI				
			manual [pixel] *	auto [pixel] *	manual [pixel]	auto [pixel]			
1°	0	East	n/a	n/a	n/a	n/a	n/a	INTERMAP5mDTM	
		North	n/a	n/a	n/a	n/a	n/a		
	1	East	0,63	n/a	0	n/a	n/a		0
		North	0,02	n/a	0	n/a	n/a		
	2	East	0,59	n/a	0,50	n/a	n/a		0
		North	0,60	n/a	0,60	n/a	n/a		
	3	East	0,56 (1,95)	0,31 (1,92)	0,52	n/a	n/a		0
		North	0,49 (0,50)	0,64 (0,64)	0,49	n/a	n/a		
	4	East	0,93 (1,70)	0,38 (1,49)	0,91	n/a	n/a		0
		North	0,81 (0,81)	0,61 (0,61)	0,81	n/a	n/a		
	4	East	0,93 (1,70)	0,38 (1,49)	0,52	n/a	n/a		ADS40
		North	0,81 (0,81)	0,61 (0,61)	0,49	n/a	n/a		
6	East	0,78 (1,24)	0,51 (1,09)	0,77	0	0	0		
	North	0,79 (0,79)	0,72 (0,72)	0,79	0	0			
9	East	n/a	n/a	n/a	0,23	0,21	0		
	North	n/a	n/a	n/a	0,62	0,47			
12	East	n/a	n/a	n/a	0,23	0,36	0		
	North	n/a	n/a	n/a	0,60	0,51			
32°	0	East	n/a	n/a	n/a	n/a	n/a	INTERMAP5mDTM	
		North	n/a	n/a	n/a	n/a	n/a		
	3	East	0,71 (1,54)	0,86 (1,52)	0,67	n/a	n/a		0
		North	1,05 (1,21)	0,46 (0,74)	1,04	n/a	n/a		
	4	East	0,81 (1,32)	0,77 (1,31)	0,79	n/a	n/a		0
		North	0,91 (1,01)	0,56 (0,70)	0,90	n/a	n/a		
	4	East	0,81 (1,32)	0,77 (1,31)	0,67	n/a	n/a		ADS40
		North	0,91 (1,01)	0,56 (0,70)	1,04	n/a	n/a		
	6	East	0,85 (1,11)	0,69 (0,99)	0,85	0,04	0,08		0
		North	0,75 (0,81)	0,52 (0,60)	0,75	0	0		
	9	East	0,80	n/a	0,80	0,98	1,66		0

12°	12	North	0,98	n/a	0,98	0,51	0,39	INTERMAP5mDTM
		East	0,78	n/a	0,78	1,00	2,43	
		North	0,95	n/a	0,95	0,48	0,42	
	0	East	n/a	n/a	n/a	n/a	n/a	
		North	n/a	n/a	n/a	n/a	n/a	
	3	East	0,44	n/a	0,35	n/a	n/a	
		North	0,38	n/a	0,38	n/a	n/a	
	4	East	0,37	n/a	0,31	n/a	n/a	
		North	0,52	n/a	0,52	n/a	n/a	
	6	East	n/a	n/a	n/a	0	n/a	
		North	n/a	n/a	n/a	0	n/a	
	9	East	n/a	n/a	n/a	0,81	n/a	
		North	n/a	n/a	n/a	0,16	n/a	
	12	East	n/a	n/a	n/a	0,83	n/a	
		North	n/a	n/a	n/a	0,24	n/a	

Table 17 - Summary of RMSEs

The following conclusions can be drawn after performing the tests according to 4.1, 4.2 using the data described in 1.1, 2, 3:

- Using the Rigorous Satellite Modeling (Toutin's Model) in PCI Geomatica OrthoEngine 2013 has been quite challenging especially for the image acquired at low elevation angle. It seems that this modelling option demands for a high number of well distributed GCPs and is very sensitive to local variations caused by registration quality in image space and/or height accuracy of reference points. In contrast to that the Rational Function Model (RFM) performed well and straight forward in both software packages, Intergraph Erdas 2013 and PCI Geomatica OrthoEngine 2013. Also the number of GCPs is not that critical as for the satellite modeling option (RFM)
- the processing speed of the orthorectification resampling process in PCI Geomatica OrthoEngine 2013 takes full advantage of modern multicore CPUs and finished processing about 10 times faster than the ERDAS process on the same PC.
- Alternative Benchmarking Method:

In order to check the usability of automatic GCP registration within a COTS environment we have tested PCI Geomatica's capabilities within OrthoEngine 2013. There are image-to-image registration tools that can only provide the ability to sample the distribution of GCPs regularly over the whole image area. To avoid specific land cover type (e.g. buildings, forest and water) as well as hilly and steep terrain it is advantageous to have more options in placing/controlling of GCPs to be extracted from reference images. PCI solves this problem by providing a tool for extracting image chips from the reference imagery - point coordinates are used. Thus the user has a full control over distribution and position within the AOI. The resulting chip database can be used as a unified reference source for future projects or when dealing with multiple images, which was in our case a big advantage while working with several acquisition dates/configurations of Kompsat-3 imagery.

The PCI solution turned out be a helpful and reliable tool for automatic GCP registration. Although the radiometric quality of the Kompsat-3 imagery have been critical due to the acquisition during winter season with sparse illumination and long cast shadows, we have

been able to find a sufficient number of good GCPs. Also the long time span between acquisition of the aerial reference orthoimage and the Kompsat-3 imagery (> 10 years) did not prevent the software from finding reliable matches. This is most likely due to the Fast Fourier Transform Phase technique (FFTP) used, which is less prone to radiometric differences between the matched images than traditional correlation techniques using Normalized Cross Correlation (NCC), which is also available in PCI but gathered less matches during our tests.

All in all the method used is less time consuming than manual GCP adaption which could also help increasing the number GCPs per scene. This is a great advantage if the images are quite different (different illumination, aerial ortho reference) as in our case and is generally a good instrument for blunder detection through over-determination during the modelling phase.

- Digital Elevation Model:

During setup of the benchmarking procedures we've discovered that the ADS40 DEM contains some potentially problematic areas. Using an illuminated version of the DEM it is evident that the DEM has been edited for a large portion of the area in order to retrieve a Digital Terrain Model (DTM). But this editing process is obviously limited to the agricultural areas of the benchmarking AOI with a rather rough and abrupt change between edited/agricultural and unedited/forested areas. Especially for satellite images with low elevation angles (e.g. the image taken on 29.11.2013 with 54° Elevation Angle) digital surface models with high spatial detail can cause unwanted resampling effects due to the following reason: low elevation observation angle causes blind spots in the image where the ground surface is hidden behind tall objects like buildings or high vegetation (due to the occluded views). When the image is orthorectified there will remain areas for which no image information has been acquired. For those areas the resampling algorithm takes the necessary information from neighbouring image pixels leading to doubling and smearing effects. Although urban areas with tall buildings are more prone to this effect it is also detectable in such rural country side areas like Maussanne test AOI.

For satellite imagery acquired at low elevation angles it is therefore generally better to use Digital Terrain Models (DTM) or alternatively Digital Surface Models (DSM) with medium resolution. Although the latter cause some loss in orthorectification accuracy the local integrity of the image for built-up and forested areas is retained.

The comparison of results for images orthorectified with the ADS40 and images retrieved using the Intermap5mDTM showed only minor differences. For the image with high elevation acquisition angle there are nearly no differences visible. Because the test with low elevation angle image showed less artefacts for built-up and tree areas when using the Intermap DTM we have decided to use this DTM for all the following test scenarios.

Requested by JRC tests using an image collected at ONA ~15deg (as GSD=0,75cm which is GSDmax that can be considered for CwRS Campaign [VHR Prime] is reached at ONA 15deg, Figure 2) will be performed after the image has been collected and the agreed scenarios are given in Table 14: Additional tests - 15deg ONA image.

All ICQ reports (Annex II) are archived in:

\\ies.jrc.it\Ho4\Common\Data\CID\MAUSSANE\KOMPSAT-3\FINAL REPORTING\ANNEX_II

References

- i. Quality Control Record – L, FWC 389.911, Version 4.0, June 11, 2014.
- ii. Kapnias, D., Milenov, P., Kay, S. (2008) Guidelines for Best Practice and Quality Checking of Ortho Imagery. Issue 3.0. Ispra
- iii. VHR image acquisition specifications for the CAP checks (CwRS and LPIS QA)-VHR profile-based specifications, Version 7.0, March 16, 2014.
- iv. <http://www.kari.re.kr> available on February 01, 2014
- v. Kompsat-3 Image Data Manual, 2014. Version 1.0.
- vi. Annex I to the Framework Contract for the supply of satellite remote sensing imagery and associated services in support to checks within the Common Agricultural Policy. Technical Specifications for the Very High Resolution profile Framework Contract (2013) Contract Notice No. 2013/S 161-280227
- vii. PCI Geomatics, (2012). Geomatica Help 2013.
- viii. <http://geospatial.intergraph.com/>
- ix. Nowak Da Costa, J., Tokarczyk P., 2010. Maussane Test Site Auxiliary Data: Existing Datasets of the Ground Control Points. The pdf file received on 06.02.2014 via FTP.
- x. Lucau, C., Nowak Da Costa J.K. (2009) Maussane GPS field campaign: Methodology and Results. Available at http://publications.jrc.ec.europa.eu/repository/bitstream/11111111/14588/1/pubsy_jrc5628_o_fmp11259_sci-tech_report_cl_jn_mauss-10-2009.pdf
- xi. Maussane test site (& geometry benchmarks). KO-Meeting-Presentation January 30, 2014.
- xii. Åstrand, J.P., Bongiorno, M., Crespi, M., Fratarcangeli, F., Nowak Da Costa, J.K., Pieralice, F., Walczynska, A. (2012). The potential of WorldView-2 for ortho-image production within the "Control with Remote Sensing Programme of the European Commission. International Journal of Applied Earth Observation and Geoinformation 19 (2012) 335–347.
- xiii. Nowak Da Costa, J.K., Walczynska, A. (2011). Geometric Quality Testing of the WorldView-2 Image Data Acquired over the JRC Maussane Test Site using ERDAS LPS, PCI Geomatics and Keystone digital photogrammetry software packages – Initial Findings with ANNEX. Available at http://publications.jrc.ec.europa.eu/repository/bitstream/11111111/22790/1/jrc60424_lb-nb-24525_en-c_print_ver.pdf
- xiv. Nowak Da Costa, J.K., Walczynska, A. (2010). Geometric Quality Testing of the Kompsat-2 Image Data Acquired over the JRC Maussane Test Site using ERDAS LPS and PCI GEOMATICS remote sensing software. Available at <http://publications.jrc.ec.europa.eu/repository/bitstream/11111111/15039/1/lbna24542enn.pdf>

- xv. Nowak Da Costa, J.K., Walczynska, A., 2010. Evaluating the WorlView-2, GeoEye-1, DMCII, THEOS and KOMPSAT-2 imagery for use in the Common Agricultural Policy Control with Remote Sensing Programme. Scientific presentation at the 16th Conference on "Geomatics in support of the CAP" in Bergamo, Italy, 24-26 November 2010. JRC Publication Management System. Available at http://mars.jrc.ec.europa.eu/mars/content/download/1998/10589/file/P4-2-Joanna_Nowak.pdf
- xvi. Grazzini, J., Astrand, P., (2013). External quality control of Pléiades orthoimagery. Part II: Geometric testing and validation of a Pléiades-1B orthoproduct covering Maussane test site. Available at <http://publications.jrc.ec.europa.eu/repository/bitstream/11111111/29229/1/lb-na-26-100-en-n.pdf>
- xvii. Grazzini, J., Lemajic, S., Astrand, P., (2013). External quality control of Pléiades orthoimagery. Part I: Geometric benchmarking and validation of Pléiades-1A orthorectified data acquired over Maussane test site. Available at <http://publications.jrc.ec.europa.eu/repository/bitstream/11111111/29541/1/lb-na-26-101-en-n.pdf>
- xviii. Grazzini, J., Astrand, P., (2013). External quality control of SPOT6. Geometric benchmarking over Maussane test site for positional accuracy assessment orthoimagery. Available at <http://publications.jrc.ec.europa.eu/repository/bitstream/11111111/29232/1/lb-na-26-103-en-n.pdf>
- xix. Fraser, C., Ravanbakhsh, M., (2009). Georeferencing of GeoEye-1 Imagery. PHOTOGRAMMETRIC ENGINEERING & REMOTE SENSING
- xx. Fraser, S., Hanley, H., Bias Compensation in Rational Functions for Ikonos Satellite Imagery. Photogrammetric Engineering & Remote Sensing Vol. 69, No. 1, January 2003, pp. 53 – 57.
- xxi. Zitova, B.,Flusser, J., (2003) Image registration methods: a survey. Image and Vision Computing 21 (2003) 977-1000.
- xxii. Lemoine, G., Giovalli, M., Geo-Correction of High-Resolution Imagery Using Fast Template Matching on a GPU in Emergency Mapping Contexts. Remote Sens. 2013, 5, 4488-4502; doi:10.3390/rs5094488
- xxiii. Tsingas, V., (1995) Operational Use and Empirical Results of Automatic Aerial Triangulation, in: D. Fritsch & D. Hobbie, Eds., 'Photogrammetric Week '95', Wichmann Verlag, Heidelberg, pp. 207-214.
- xxiv. Xiong, Z. (2009). Technical Development for Automatic Aerial Triangulation of High Resolution Satellite Imagery. Ph.D. dissertation, Department of Geodesy and Geomatics Engineering, Technical Report No. 268, University of New Brunswick, Fredericton, New Brunswick, Canada, 302 pp.
- xxv. Fonseca L., Majunath, B., (1996) Registration Techniques for Multisensor Remotely Sensed Imagery. Photogrammetric Engineering & Remote Sensing, Vol. 62, No. 9, September 1996, pp. 1049-105

ANNEX I to the New sensor benchmark report on Kompsat-3

EXTERNAL QUALITY CONTROL OF KOMPSAT-3 ORTHOIMAGERY REPORT

Contents

1.	Method for external quality checks of ortho images.....	4
1.1	Independent check points (ICPs) - selection, distribution and registration	4
1.2	Geometric quality assessment – measurements and calculations	7
2.	Outcome and discussion about ECO	8
2.1	Overall results	8
2.2	Discussion on off-nadir angle factor	13
2.3	Discussion on software usage factor	15
2.4	Discussion on Rigorous and Rational Function Modelling.....	16
2.5	Discussion on the number of GCPs used for the modelling.....	18
3.	Discussion about the alternative and standard benchmarking methodology	19
4.	Discussion about DEM ADS ₄₀ and INTERMAP _{5m} DTM.....	20
4.1	Comparison between DEM ADS ₄₀ and INTERMAP 5m DTM and their potential influence on the final geometric accuracy of the orthoimage.....	20
4.2	Visual quality comparison of orthoimages produced using DEM ADS ₄₀ and INTERMAP 5 DTM.....	23
5.	Additional test of 12° off nadir angle scene	24
6.	Conclusions.....	27
7.	Additional comments.....	28

List of tables

Table 1: Identical check points specifications	4
Table 2: ICPs overview for each ortho image	6
Table 3: Results of RMSE _{1D} measurements in JRC ICPs dataset.	8
Table 4: Results of RMSE _{1D} measurements in JRC ICPs dataset.	9
Table 5: Results of RMSE _{1D} measurements in JRC ICPs dataset.	24

List of figures

Figure 1: ICPs dataset used by JRC in the EQC of Kompsat-3 ortho imagery.	4
Figure 2: Example of the ICP localization on the orthoimage – “difficult case”.	5
Figure 3: Comparison of RMSEs using standard and alternative weighting parameters - 1° off nadir	10
Figure 4: Comparison of RMSEs using standard and alternative weighting parameters - 32° off nadir	10
Figure 5: Point representation of all planimetric RMSE _{1D} errors measured in JRC ICPs dataset.	11
Figure 6: Residuals measured on Kompsat-3 orthoimage (1°) with standard and alternative weighting GCP parameters.	11
Figure 7: Residuals measured on Kompsat-3 orthoimage (32°) with standard and alternative weighting GCP parameters.	12
Figure 8: Graph of average RMSEs as a function of the number of GCPs and off nadir angle	13
Figure 9: Measured RMSEs as a function of the used method and off nadir angle.	14
Figure 10: Behaviour of RMSEs across the various number of GCPs for PCI and ERDAS software	15
Figure 11: Graph representation of RMSEs comparison between Tutin’s Rigorous and RPC model.	16
Figure 12: 1-D RMSEs measured on the orthoimages derived using RPC and rigorous model, as a function of the number of GCPs used for modelling.	17
Figure 13: 1-D RMSE measured on the Rigorous-based orthoimages as a function of the number of GCPs.	18
Figure 14: 1-D RMSE measured on the orthoimages as a function of the number of GCPs used for the modelling, with the focus on each GCPs detection methodology (and software)	19
Figure 15: 1-D RMSE comparison between the orthoimages processed with ADS40 and orthoimages processed with INTERMAP5mDTM	21
Figure 16: 1-D RMSE measured on orthoimages as a function of methodologies used for ortho production. ...	21
Figure 17: Visual quality comparison between DEM ADS40 and INTERMAP5mDTM usage	23
Figure 18: 1-D RMSE measured on the orthoimages as a function of the number of GCPs used for the modelling.	25
Figure 19: Comparison of RMSEs for 3 and 4 GCPs (RPC), using PCI and ERDAS software	25
Figure 20: Graph of RMSEs as a function of the number of GCPs and off nadir angle - RPC model.	25
Figure 21: Graph of RMSEs as a function of the number of GCPs and off nadir angle	26

This external quality control (EQC) report on the KOMPSAT-3 optical satellite ortho-product is a part of the "New sensor benchmark report on Kompsat-3". References in this annex therefore refer to the concrete chapters of that report which is in this context called just the "benchmarking report" or to its list of references.

JRC as an independent entity performs a validation phase of the benchmarking workflow methodology used for verifying of a satellite's ortho-product compliance with the geometric quality criteria set up for the Control with Remote Sensing program (CwRS), in Common Agriculture Policy (CAP). The workflow follows the Guidelines for Best Practice and Quality Checking of Ortho Imagery (Kapnias et al., 2008) [ii] and is in detail described in the chapter 4. Methodology (benchmarking report) or [xv], [xvi], [xvii].

The report therefore summarizes the results coming from the detailed geometric quality assessment of the Kompsat-3 orthoimagery (precisely 74 orthos altogether) derived from two Kompsat-3 scenes (Level 1R) captured under three different viewing angles (1° , 12° and 32° off nadir angle).

The tested orthoimages were provided by the Framework (FW) Contractor European Space Imaging GmbH who subcontracted their production to GAF AG.

The sensor orientation and the orthorectification process were carried out with PCI Geomatics 2013, Intergraph ERDAS 2013 software, using both Rigorous model and Rational Polynomial Functions (RPFs) model with Rational Polynomial Coefficients (RPCs), various number of ground control points (GCPs) and two different methodologies for GCPs selection. For further explanation and details see the chapter 4 Methodology (benchmarking report).

The main objectives of the geometric accuracy assessment are as follows:

1. To determine whether the orthorectified imagery of Kompsat-3 sensor complies with the accuracy criteria defined for CwRS, in CAP and consequently whether the optical sensor can be qualified for the following profiles:
 - a) A1.VHR prime profile ($1D$ RMSE $<2m$), spatial resolution requirements: $GSD \leq 0.75m$ (PAN, PSH) and $GSD \leq 3m$ (MSP)
 - b) E. VHR backup profile ($1D$ RMSE $<5m$), spatial resolution requirements: $GSD \leq 3m$ (PAN, PSH) and $GSD \leq 12m$ (MSP)
2. To assess the influence of various factors (off-nadir angle of a scene, number of GCPs, software etc., see chapter 2) entering into the satellite image orientation and orthorectification phase on the final horizontal accuracy of ortho products.
3. To compare the proposed alternative benchmarking methodology with the standard one.
4. To compare INTERMAP 5m DTM and DSM ADS40, their influence on the geometric quality of the final orthoimage.

1. Method for external quality checks of ortho images

The method for the external quality checks strictly follows the Guidelines for Best Practice and Quality Checking of Ortho Imagery (Kapnias et al., 2008) [ii].

1.1 Independent check points (ICPs) - selection, distribution and registration

For the evaluation of the geometric accuracy of the Kompsat-3 ortho imagery, 20 to 26 independent ICPs were selected by a JRC operator. Both GCPs and ICPs were retrieved from already existing datasets of differential global positioning system (DGPS) measurements over Maussane test site. These datasets are updated and maintained by JRC. Considering the accuracy, distribution and recognisability on the given images, points from the four datasets were decided to be used for the EQC. The intention was to spread the points evenly across the whole image while keeping at least the minimum recommended number of 20 points (Kapnias et al., 2008). JRC for the location of the ICPs took into account the distribution of the GCPs determined by the FW Contractor and provided to JRC together with the products. Since the measurements on ICPs have to be completely independent (i.e. ICP must not correspond to GCP used for correction) GCPs taken into account in the geometric correction have been excluded from the datasets considered for EQC.

Regarding the positional accuracy of ICPs, according to the Guidelines (Kapnias et al., 2008)[ii] the ICPs should be at least 3 times (5 times recommended) more precise than the target specification for the ortho, i.e. in our case of a target 2.0m RMS error the ICPs should have a specification of 0.65m (0.40m recommended). All ICPs that have been selected fulfil therefore the defined criteria (Table 1).

Dataset	RMSE _x [m]	RMSE _y [m]	Number of points
ADS40 GCP_dataset_Maussane 2003	0,05	0,10	1
VESEL_GCP_dataset_Maussane 2005	0,49	0,50	8
Multi-use_GCP_dataset_Maussane	0,30	0,30	15
Maussane GNSS field campaign 2012	< 0,15	< 0,15	2

Table 1: Identical check points specifications

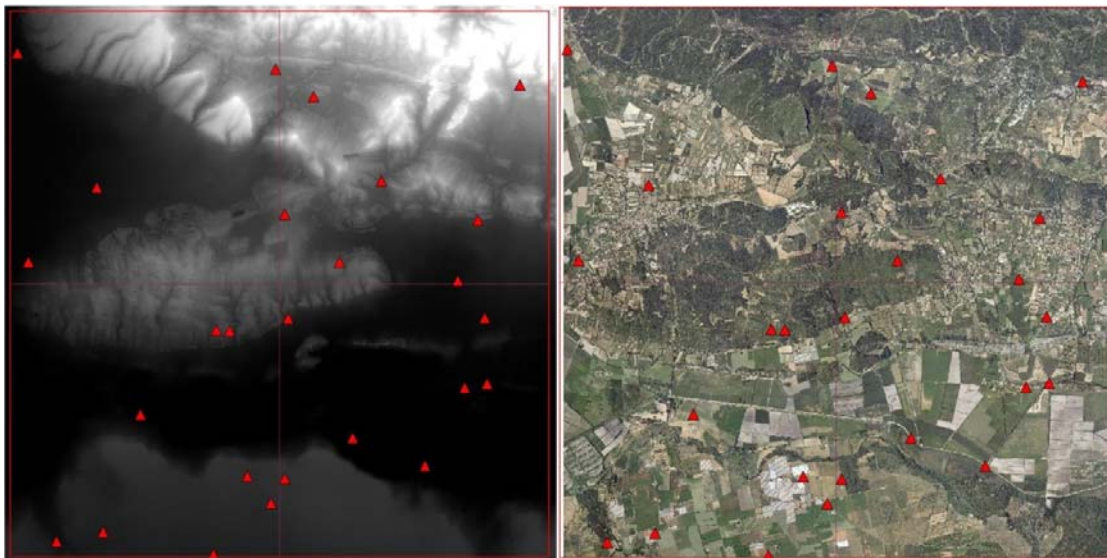


Figure1: ICPs dataset used by JRC in the EQC of Kompsat-3 ortho imagery.

Left: ICPs displayed over the ADS40 DEM. Right: ICPs are displayed over the UltraCam acquisition of Maussane.

Since the datasets of DGPS points are of a high variety as for the date of origin is concern (2003-20012) many points could not have been detected due to the meanwhile change of the overall landscape. Also the ADS40 aerial orthomosaic is 11 years old and therefore does not always correspond to the actual state of the region. Thus for the selection of some ICPs on the orthoimages the other complementary sources to the aerial image were used, like for instance previously orthorectified VHR images (PLA) or Google Earth 2D sequences, which helps to follow the change of the situation during the years, for some cases (where available) also 3D view.



Figure2: Example of the ICP localization on the orthoimage – “difficult case”

From up to down: 1. Row: aerial orthomosaic imagette (2004), photo of the point measurement(2005), additional auxiliary image of Pleiades(2013), 2. Row: Google Earth sequence of images 2004, 2008, 2010, 3 Row: Kompsat-3 ortho product-1° off nadir angle, Kompsat-3 ortho product-32° off nadir angle

ANNEX I - External quality control of Kompsat-3 orthoimagery

ID	E [m]	N [m]	0 GCPs		3 GCPs		4 GCPs		6 GCPs		9 GCPs		12 GCPs	
			Off-nadir angle											
			1°	32°	1°	32°	1°	32°	1°	32°	1°	32°	1°	32°
66004	636363,62	4846077,515	x	x	x	x	x	x	x	x	x	x	x	x
66005	641149,126	4845775,194	x	x	x	x	x	x	x	x	x	x	x	x
66009	641850,726	4845276,823	x	x	x	x	x	x	x	x	x	x	x	x
66014	645687,638	4845487,947	x	x	x	x	x	x	x	x	x	x	x	x
66022	637947,945	4837300,701	x	x	x	x	x	x	x	x	x			
66023	640624,493	4838320,517	x	x	x	x	x	x	x	x	x	x	x	x
66024	641320,704	4838276,563	x	x	x	x	x	x	x	x	x	x	x	x
66025	641380,518	4841215,071	x	x	x	x	x	x	x	x				
66026	640049,047	4840996,065	x	x	x	x	x	x	x	x	x	x	x	x
66028	640296,274	4840992,691	x	x	x	x	x	x	x	x	x	x	x	x
66031	644655,956	4839947,667	x	x	x	x	x	x	x	x	x	x	x	x
66038	644535,092	4841910,055	x	x	x	x	x	x	x	x	x	x	x	x
66044	641321,746	4843119,664	x	x	x	x	x	x	x	x	x	x	x	x
66045	642336,27	4842251,705	x	x	x	x	x	x	x	x	x	x	x	x
66049	644906,913	4843017,779	x	x	x	x	x	x	x	x	x	x	x	x
110016	638647,342	4839449,608	x	x	x	x	x	x	x	x	x			
440009	643112,409	4843729,238	x	x	x	x	x	x	x	x	x			
440011	636560,472	4842244,515	x	x	x	x	x	x	x	x	x	x	x	x
440015	645030,5	4841227,208	x	x	x	x	x	x						
440019	642578,11	4839029,461	x	x	x	x	x	x	x	x	x	x	x	x
440021	637082,024	4837127,366	x	x	x	x	x	x	x	x	x	x	x	x
440022	640003,541	4836888,216	x	x	x	x	x	x	x	x	x	x	x	x
440023	641060,734	4837826,921	x	x	x	x	x	x	x	x	x	x	x	x
440024	643930,013	4838510,152	x	x	x	x	x	x	x	x	x	x	x	x
C2R4	637829,72	4843609,87	x		x		x		x		x		x	
C4R5	645079,24	4840015,39	x	x	x	x	x	x	x	x	x	x	x	x

Table 2: ICPs overview for each ortho image

The projection and datum details of the above mentioned data are UTM 31N zone, WGS 84 ellipsoid.

1.2 Geometric quality assessment – measurements and calculations

Geometric characteristics of orthorectified images are described by Root-Mean-Square Error (RMSE) $RMSE_x$ (easting direction) and $RMSE_y$ (northing direction) calculated for a set of Independent Check Points.

$$RMSE_{1D}(East) = \sqrt{\frac{1}{n} \sum_{i=1}^n (X_{REG(i)} - X_{(i)})^2} \qquad RMSE_{1D}(North) = \sqrt{\frac{1}{n} \sum_{i=1}^n (Y_{REG(i)} - Y_{(i)})^2}$$

where $X, Y_{REG(i)}$ are ortho imagery derived coordinates, $X, Y_{(i)}$ are the ground true coordinates, n express the overall number of ICPs used for the validation.

This geometric accuracy representation is called the positional accuracy, also referred to as planimetric/horizontal accuracy and it is based on measuring the residuals between coordinates detected on the orthoimage and the ones measured in the field or on a map of an appropriate accuracy.

Unlike the values obtained from the field measurements (in our case with GPS device) which are of the defined accuracy the coordinates registered from the involved orthoimages are biased by various influencing factors (errors of the source image, quality of auxiliary reference data, visual quality of the image, experience of an operator etc..). It should be taken into account that all these factors are then subsequently reflected in the overall RMSE which in practice aggregates the residuals into a single measure.

All measurements presented in this annex were carried out in Integrgraph ERDAS Imagine 2010 software, using Metric Accuracy Assessment tool for quantitatively measuring the accuracy of an image which is associated with a 3D geometric model. Protocols from the measurements contain other additional indexes like mean errors or error standard deviation that can also eventually help to better describe the spatial variation of errors or to identify potential systematic discrepancies. (Kapnias et al., 2008)[ii].

2. Outcome and discussion about ECO

2.1 Overall results

PCI Geomatics 2013 (standard parameters)			RPC			Rigorous		DEM
Off-nadir angle	Number of GCPs	Direction	PCI manual [m]	auto [m]	Erdas manual [m]	PCI manual [m]	auto [m]	
1°	0	East	28,56	n/a	28,60	n/a	n/a	INTERMAP _{5m} DTM ADS ₄₀
		North	8,88	n/a	8,89	n/a	n/a	
	3	East	2,25	1,97	1,14	n/a	n/a	
		North	1,30	0,93	1,04	n/a	n/a	
	4	East	1,60	1,61	0,96	n/a	n/a	
		North	1,19	1,01	1,13	n/a	n/a	
	6	East	1,57	1,65	0,96	n/a	n/a	
		North	1,21	0,99	1,10	n/a	n/a	
	9	East	1,39	1,65	0,89	0,87	1,25	
		North	1,06	0,96	0,97	0,83	1,54	
	12	East	n/a	n/a	n/a	1,12	1,24	
		North	n/a	n/a	n/a	0,9	1,11	
32°	0	East	48,55	n/a	48,20	n/a	n/a	INTERMAP _{5m} DTM ADS ₄₀
		North	6,88	n/a	6,82	n/a	n/a	
	3	East	2,14	3,09	2,12	n/a	n/a	
		North	1,03	1,28	1,00	n/a	n/a	
	4	East	2,83	2,46	1,86	n/a	n/a	
		North	1,01	1,58	1,05	n/a	n/a	
	6	East	3,10	2,67	2,00	n/a	n/a	
		North	0,96	1,52	0,99	n/a	n/a	
	9	East	2,22	2,21	1,52	3,74	3,81	
		North	0,92	1,25	1,40	1,18	1,19	
	12	East	n/a	n/a	n/a	2,12	2,70	
		North	n/a	n/a	n/a	1,29	1,34	
12	East	n/a	n/a	n/a	2,23	2,43		
	North	n/a	n/a	n/a	1,32	1,48		

Table 3: Results of RMSE_{1D} measurements in JRC ICPs dataset.

The results are presented altogether for the different input viewing angles, software, GCP collection method, 3D geometric correction method and different DEM used for orthorectification process modelling. The highest and lowest errors measured (per row) are marked with red and blue colours respectively. The values highlighted with the red font exceed the set value for the VHR prime profile (RMSE of 2m). In PCI Geomatica 2013 – RPC modelling – the standard accuracy values for GCPs were used.

ANNEX I - External quality control of Kompsat-3 orthoimagery

PCI Geomatics 2013 (alternative weighting parameters)			RPC			Rigorous		DEM	
			PCI		Erdas	PCI			
			manual [m]	auto [m]	manual [m]	manual [m]	auto [m]		
Off-nadir angle	Number of GCPs	Direction							
1°	0	East	28.56	n/a	28.60	n/a	n/a	INTERMAP5mDTM	
		North	8.88	n/a	8.89	n/a	n/a		
	1	East	1.96	n/a	1.57	n/a	n/a		
		North	0.95	n/a	1.00	n/a	n/a		
	2	East	1.35	n/a	1.19	n/a	n/a		
		North	1.16	n/a	1.01	n/a	n/a		
	3	East	1.20	1.04	1.14	n/a	n/a		
		North	1.08	0.97	1.04	n/a	n/a		
	4	East	0.93	0.92	0.96	n/a	n/a		
		North	1.14	0.99	1.13	n/a	n/a		
	6	East	0.96	0.95	0.96	n/a	n/a		ADS40
		North	1.20	0.98	1.10	n/a	n/a		
9	East	0.89	1.01	0.89	0.87	1.25			
	North	1.02	1.02	0.97	0.83	1.54			
12	East	n/a	n/a	n/a	1.12	1.24			
	North	n/a	n/a	n/a	0.9	1.11			
32°	0	East	48.55	n/a	48.20	n/a	n/a	INTERMAP5mDTM	
		North	6.88	n/a	6.82	n/a	n/a		
	3	East	2.27	2.02	2.12	n/a	n/a		
		North	1.03	1.07	1.00	n/a	n/a		
	4	East	1.97	1.57	1.86	n/a	n/a		
		North	0.89	1.35	1.05	n/a	n/a		
	6	East	2.10	1.75	2.00	n/a	n/a		ADS40
		North	0.87	1.26	0.99	n/a	n/a		
	9	East	0.92	1.58	1.52	3.74	3.81		
		North	1.29	1.22	1.40	1.18	1.19		
	12	East	1.4	n/a	1.28	2.12	2.70		INTERMAP5mDTM
		North	0.96	n/a	0.95	1.29	1.34		
12	East	1.26	n/a	1.23	2.23	2.43			
	North	0.97	n/a	0.96	1.32	1.48			

Table 4: Results of RMSE_{1D} measurements in JRC ICPs dataset.

The results are presented altogether for the different input viewing angles, software, GCP collection method, 3D geometric correction method and different DEM used for orthorectification process modelling. The highest and lowest errors measured (per row) are marked with red and blue colours respectively. The values highlighted with the red font exceed the set value for the VHR prime profile (RMSE of 2m). Please note that the values for the Erdas software and for the rigorous model are the same as in the Table 3 In PCI Geomatica 2013 – RPC modelling – the weighting accuracy values for GCPs were used.

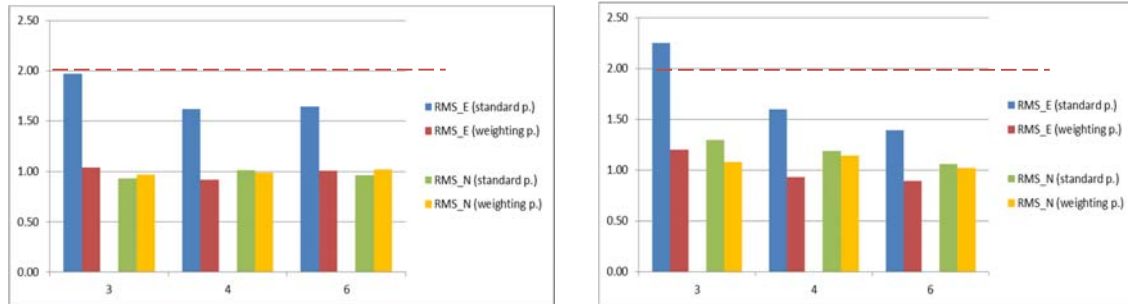


Figure3: Comparison of RMSEs using standard and alternative weighting parameters - 1° off nadir

Standard parameters (blue, green) and alternative weighting PCI parameters (red, yellow). From left to right: automatic selection of GCPs (PCI Geomatics 2013, Intermap5mDTM), manual detection of GCPs (PCI Geomatics 2013, Intermap5mDTM)

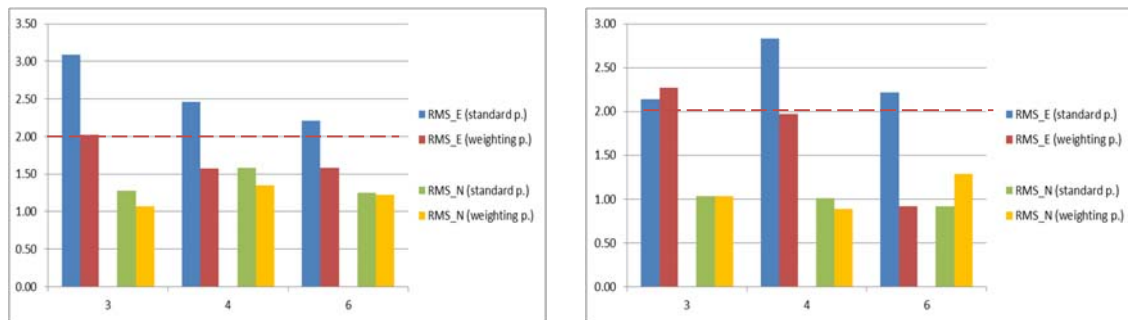


Figure4: Comparison of RMSEs using standard and alternative weighting parameters - 32° off nadir

Standard parameters (blue, green) and alternative weighting PCI parameters (red, yellow). From left to right: automatic selection of GCPs (PCI Geomatics 2013, Intermap5mDTM), manual detection of GCPs (PCI Geomatics 2013, Intermap5mDTM)

A detailed explanation for using standard/alternative weighting accuracy parameters for GCPs in PCI Geomatics 2013 software can be found in the chapter 4.3 Sensor Alignment issue (benchmarking report)

Looking at the charts representing comparison between RMSEs of derived ortho products using both standard and weighting accuracy values for GCPs, we can summarise following conclusions:

- Testing the orthorectified images derived using the 1° off nadir angle scene and alternative weighting values the RMSEs in the Easting direction rapidly decreased in comparison to the standard values. The maximal RMSE changed from 2.25m to 1.20m. Regarding the Northing direction the change of the accuracy values for GCPs did not significantly influence the RMSEs. Where the GCPs were detected manually we can observe a little decrease.
- Testing the orthorectified images derived using the 32° off nadir angle scene and the alternative PCI parameters the RMSEs in the Easting direction also decreased in comparison to the standard values, but for 3 GCPs remaining still high (above or just at the limit of 2m). Using the manual detection of GCPs even 4 GCPs still do not give really satisfactory results (around 2m).

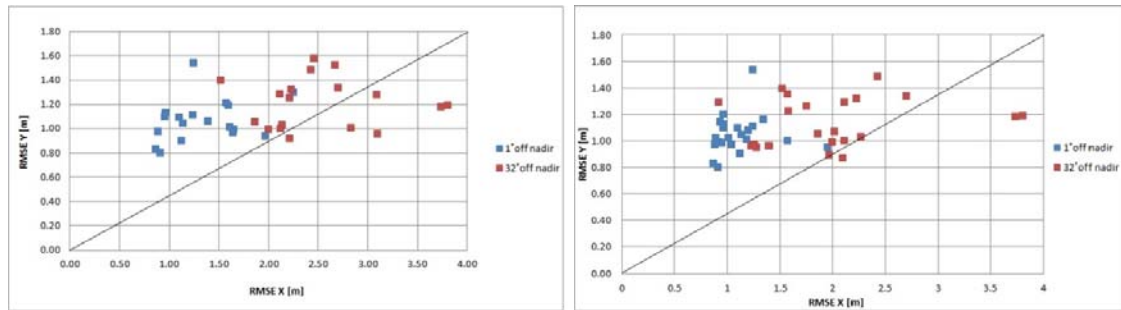


Figure5: Point representation of all planimetric $RMSE_{1D}$ errors measured in JRC ICPs dataset

From left to right: RMSE values resulted from the standard parameters, RMSE values resulted from the alternative weighting parameters (the numbers differentiate for PCI software - RPC method, for the rest (Erdas both RPC and Rigorous model, PCI rigorous model) remain the same as the method (images) did not change. Right chart contains additional data (1GCP, 2GCPs for 1° off nadir angle (both Erdas and PCI software) and 9GCPs, 12GCPs for 32° off nadir angle (both Erdas and PCI software), see the chapter 4.4 Additional tests (benchmarking report)

The

Figure5 confirms the overall better results of RMSEs when the alternative method was used. The high values of RMSEs in the Easting direction (RMSE X) that remained in the right chart for 32° off nadir angle are results of the rigorous model application during the sensor orientation phase.

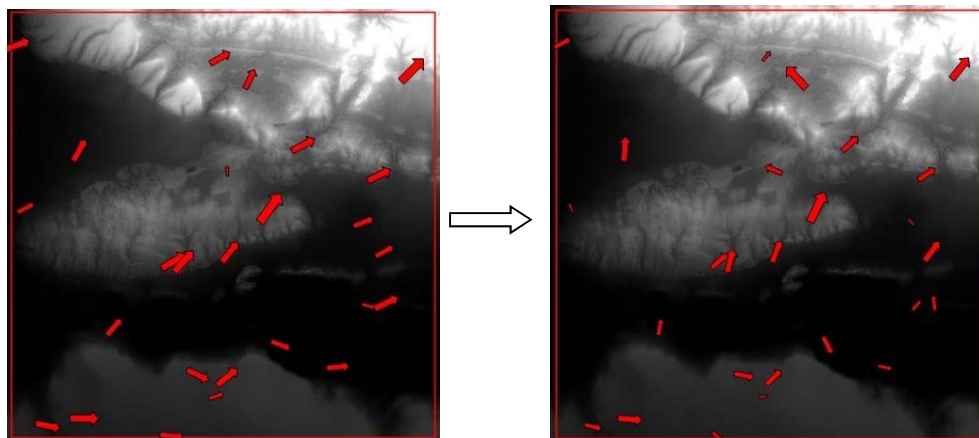


Figure6: Residuals measured on Kompsat-3 orthoimage (1°) with standard and alternative weighting GCP parameters.

The 2D residuals are represented over the ICPs as red arrows – their turnings indicate shifts' directions, the value of the shift is displayed by the size of the arrow. Left: Orthoimage produced using 1° off nadir angle image, 4GCPs, INTERMAP5mDTM, manual GCP selection and standard GCP parameters. Right: Orthoimage produced using 1° off nadir angle image, 4GCPs, INTERMAP5mDTM, manual GCP selection and alternative weighting GCP parameters.

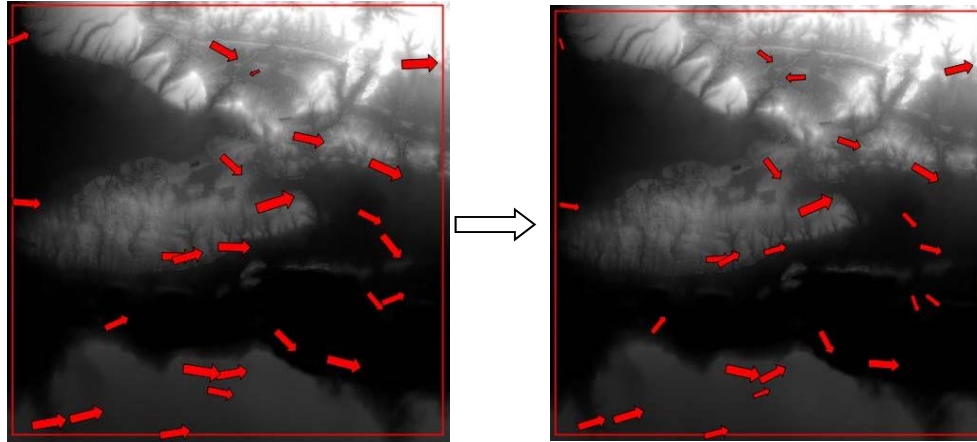


Figure7: Residuals measured on Kompsat-3 orthoimage (32°) with standard and alternative weighting GCP parameters.

The 2D residuals are represented over the ICPs as red arrows – their turnings indicate shifts' directions, the value of the shift is displayed by the size of the arrow. Left: Orthoimage produced using 32° off nadir angle image, 4GCPs, INTERMAP₅mDTM, manual GCP selection and standard GCP parameters. Right: Orthoimage produced using 32° off nadir angle image, 4GCPs, INTERMAP₅mDTM, manual GCP selection and alternative weighting GCP parameters.

Taking into account the analysis above and the conclusions made, it was decided that for the further geometric assessments and discussions only the results (concerning PCI Geomatics 2013 - RPC modelling), coming from the alternative weighting accuracy values for GCPs applied in the modelling phase, will be considered.

2.2 Discussion on off-nadir angle factor

In general, it can be concluded that 1-D RMS errors are sensitive to the overall off nadir angle of the acquired scene. The increase with the increasing off nadir angle is observed.

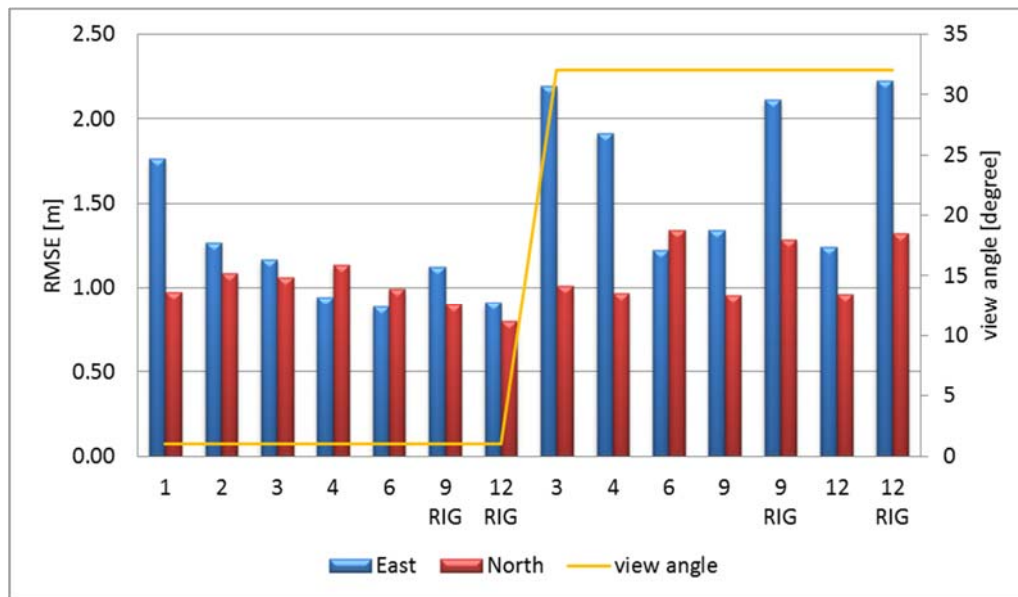
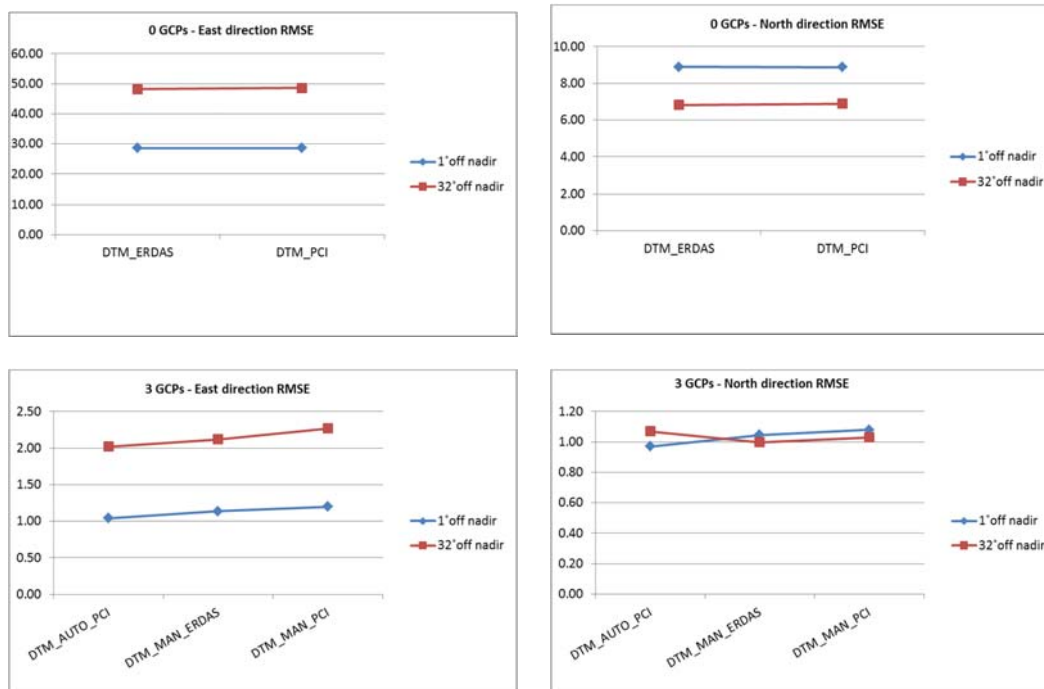


Figure8: Graph of average RMSEs as a function of the number of GCPs and off nadir angle
 The comparison is done for the orthoimages derived with INTERMAP5mDTM, the manual method of GCPs selection, both RPC and rigorous model

For the 1-D RMS errors measured in the Easting direction the off nadir angle influence is clear and substantial through all GCPs models. As for the Northing direction is concerned the variance is not so visible when the RPC modelling is used, the results are more equilibrated between each other. However the tendency of big differences still appears for the products where the rigorous model was applied, see Figure9.



ANNEX I - External quality control of Kompsat-3 orthoimagery

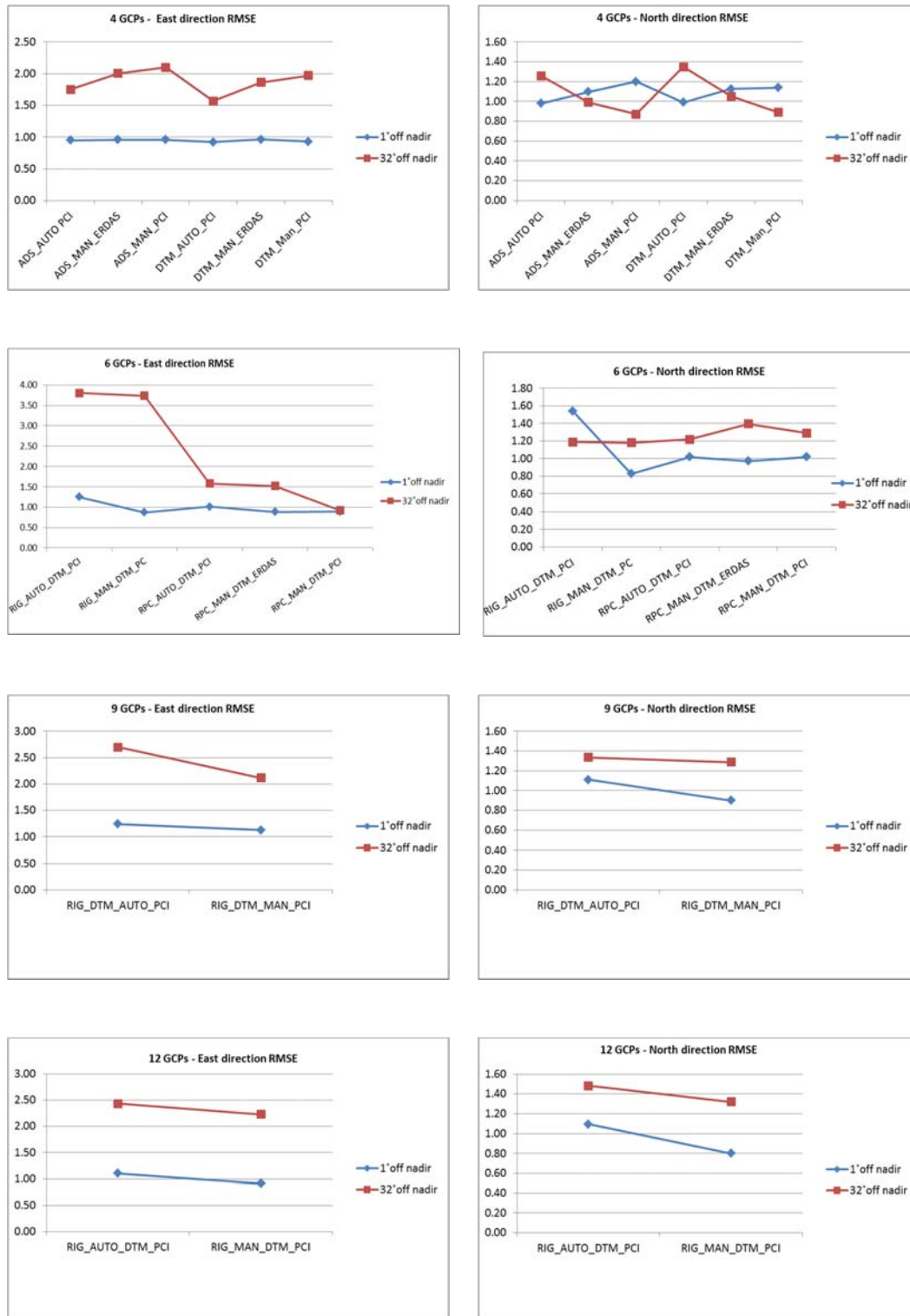


Figure: Measured RMSEs as a function of the used method and off nadir angle
 From up to down : 0-12 GCPs, from left to right: Easting , Northing direction respectively. For the simplicity the following abbreviations are used: RIG= rigorous model, RPC= RPC model, AUTO,MAN= automatic, manual selection of GCPs, ADS= DEM ADS₄₀, DTM= INTERMAP₅MDTM

2.3 Discussion on software usage factor

To compare algorithms implemented in different COTS, ERDAS IMAGINE 2013, and PCI Geomatica 2013 software were selected to derive the corresponding ortho products from the acquired images. From the Figure10 could be concluded the following:

- Concerning RMSEs in the Northing direction both software give very comparable results independently on the viewing angle of images.
- RMSEs in the Easting direction for the low off nadir angle image differ for each software when only few GCPs enter into the production. In that case ERDAS software provides better results. However when more than 2 GCPs are used the software performance concerning the RMSEs is equal.
- RMSEs in the Easting direction for the high off nadir angle image are the same for both software with the exception of 6 GCPs. At this point a kind of anomaly in the PCI RMSEs behaviour could be seen since the RMSE for this case extremely decreased.

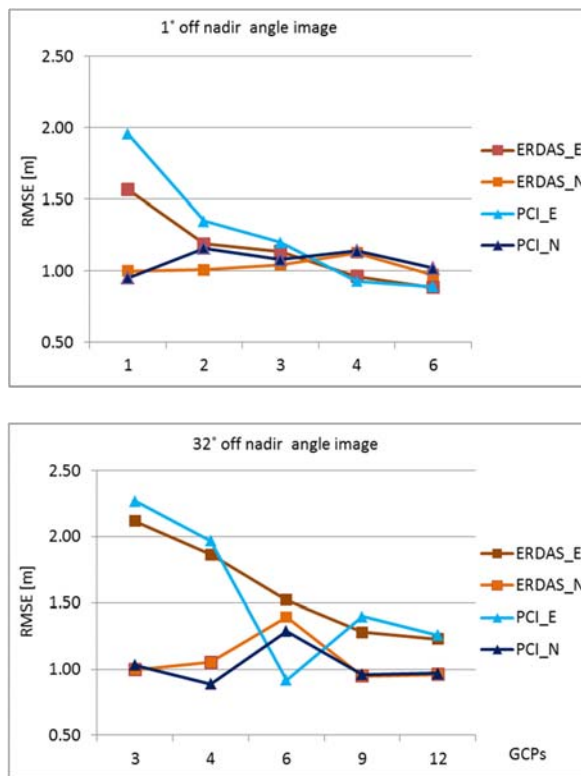


Figure10: Behaviour of RMSEs across the various number of GCPs for PCI and ERDAS software

From up to down: 1° off nadir, 32° off nadir angle image respectively. For better comparison the same methodology for the production of ortho products was selected (IntermapsDTM, RPC function model, manual method of GCPs selection)

As a conclusion we can say that when more than 2 GCPs are used in the production of orthoimages both software give basically the same results.

2.4 Discussion on Rigorous and Rational Function Modelling

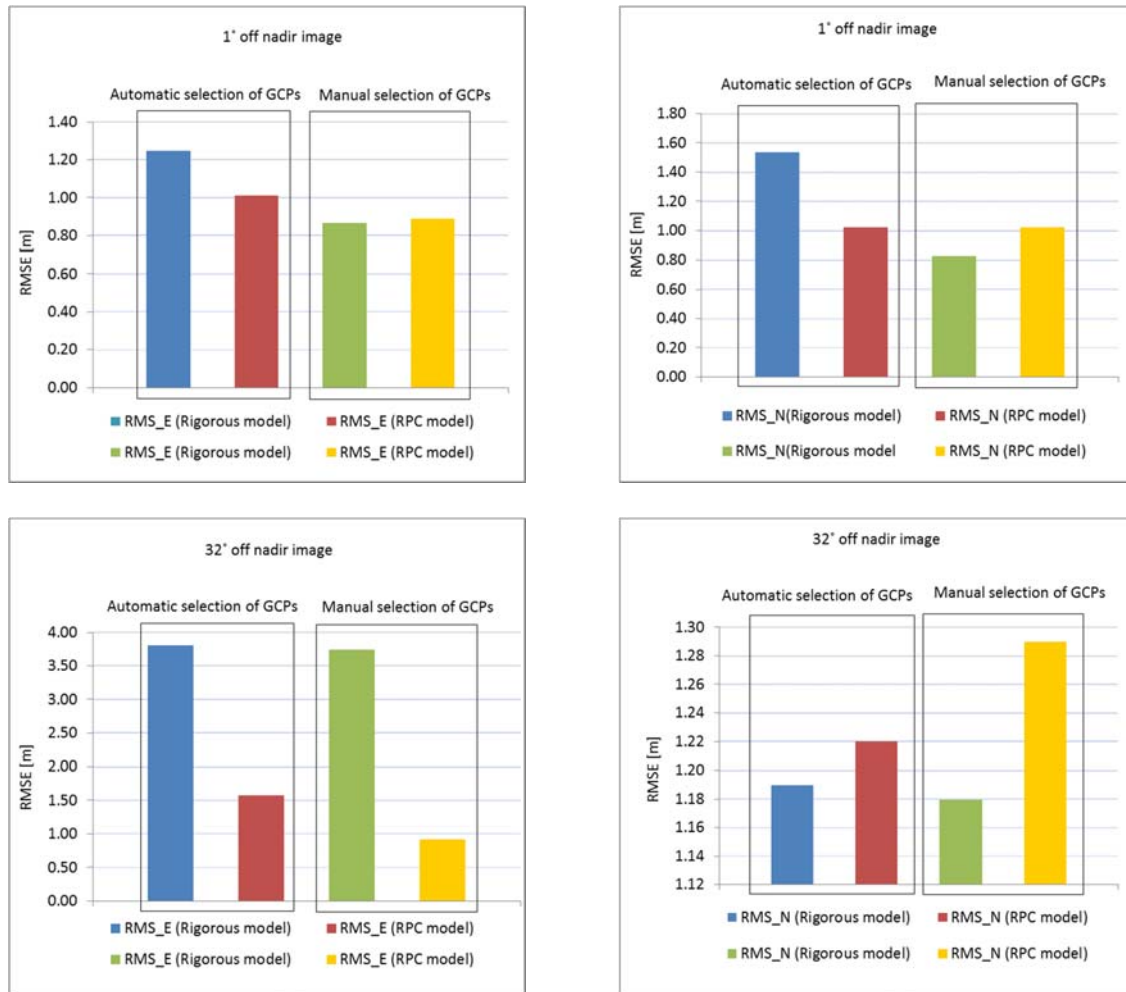


Figure11: Graph representation of RMSEs comparison between Tutin’s Rigorous and RPC model
 Graphs compare the RMSEs measured on the orthoimages produced by different modelling methods but using always 6 GCPs. The comparison considers GCPs detection method (blue x red for automatic selection, green x yellow for manual selection) and viewing angle. From up to down - left to right: 1° off nadir angle - RMSEs in the Easting, Northing direction, 32° off nadir angle - RMSEs in the Easting, Northing direction

Comparing the results displayed in the Figure11 we can summarise the following findings:

- In general, the RMSE values for both models (Rigorous and RPC) are sensitive to the overall off nadir angle, with increasing off nadir angle increase also their values. The huge, non-standard increase of RMSEs in the easting direction for the rigorous modelling is reaching the 2.87m.
- The rigorous modelling seems to be more prone to the GCPs selection method, the manual method appears to give better results than the automatic selection.
- The RMS errors measured on the orthoimages derived from the 1° off nadir angle scene confirm better results for the RPC model compare to the rigorous one when automatic selection of GCPs is applied. Very similar performance for both models is achieved applying the standard GCPs selection methodology.

- Measuring the RMS errors on the orthoimages derived from the 32° off nadir angle scene shows big differences (around 2.5m) in the Easting direction between the rigorous and RPC modelling. The rigorous modelling gives bad results with the maximal RMSE (East) over 3.50 m. The values of the RMSE in the Northing direction are more similar to each other for both models and the GCPs collection methods.

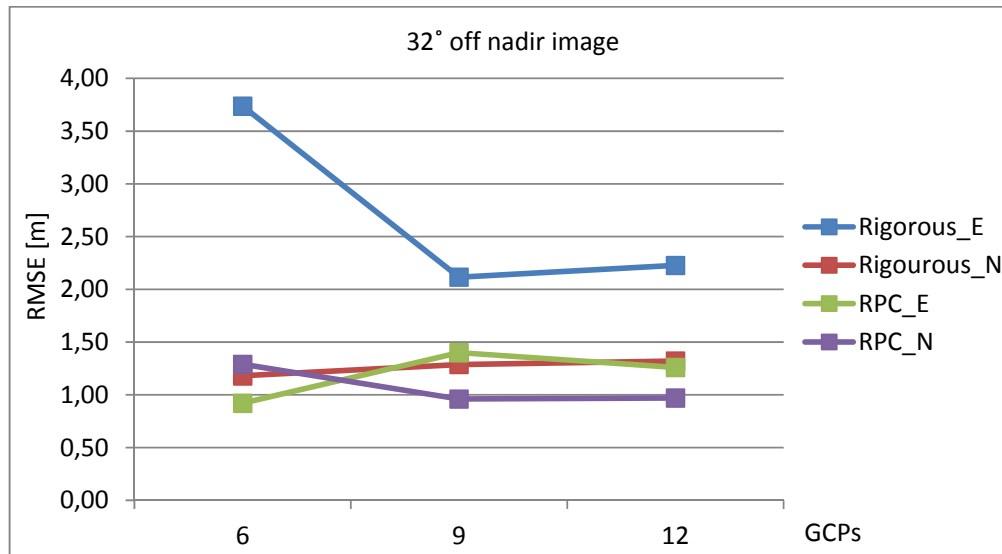


Figure12: 1-D RMSEs measured on the orthoimages derived using RPC and rigorous model, as a function of the number of GCPs used for modelling

The Figure12 illustrates the performance of each model for a various number of GCPs present in the modelling, in this case considering only the 32° off nadir angle scene. The rigorous modelling provides constantly worse RMSE values compare to RPC based modelling. From 9 GCPs onwards the number of GCPs does not improve the performance of the models.

2.5 Discussion on the number of GCPs used for the modelling

Looking at the Figure10,

Figure13 and Figure14 we can summarise the following findings:

- While the RMSEs in the Easting direction measured on the orthoimages derived from 1° off nadir angle scene, using the RPC model, are sensitive to the number of GCPs (lower RMSE with higher number of GCPs), the RMSEs in the Northing direction have a steady trend regardless the increasing number of GCPs. The same can be said for the orthoimages derived from the 32° off nadir angle image, using RPC model, except for the situation when 6 GCPs were used. As already mentioned above this case somewhat differentiates from the overall RMSEs tendency.

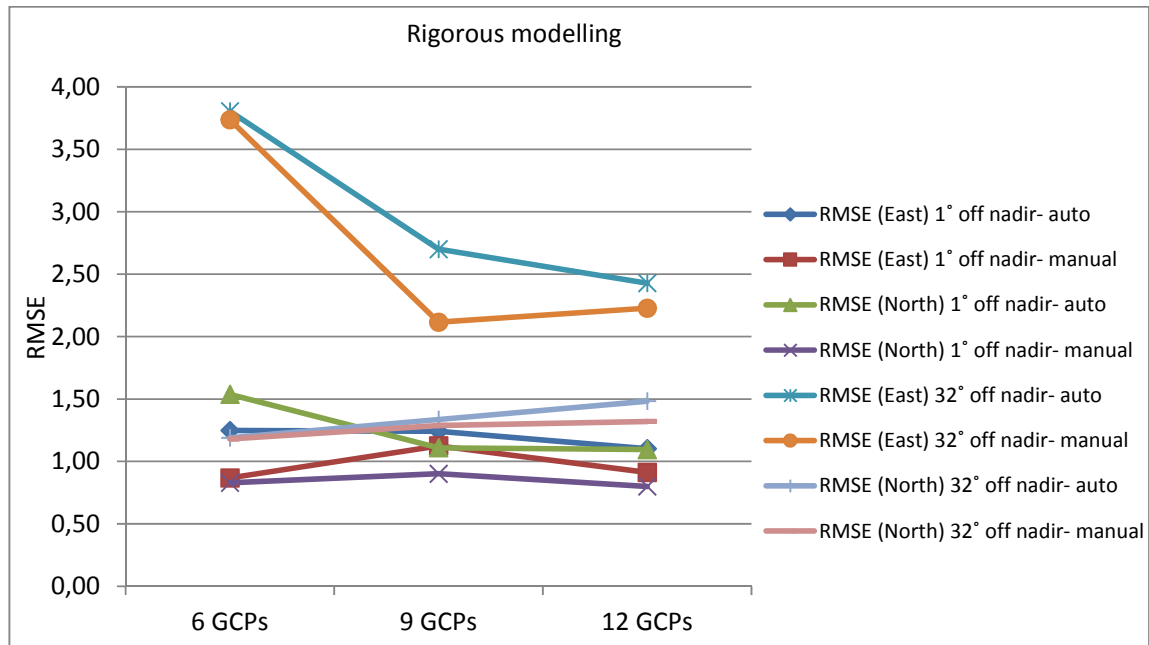


Figure13: 1-D RMSE measured on the Rigorous-based orthoimages as a function of the number of GCPs

- Applying the rigorous model, there is no clear correlation between the measured RMSEs and the number of GCPs used for the modelling. An exception is RMSEs (East), for the 32° off nadir angle scene, where a significant decrease (1.5m) is observed while going from 6 GCPs to 9 GCPs.

3. Discussion about the alternative and standard benchmarking methodology

The FW contractor pointed out the alternative possibility of the benchmarking method based on the automatic selection of GCPs using an image registration function also called image-to image correlation technique, more described in the chapter 4.2 Alternative Benchmarking Method (benchmarking report) or [xix], [xx], [xxi], [xxv]. It was therefore decided to make a comparison test between this alternative methodology and the standard one (manual selection of GCPs) in order to estimate its usability and a possible implication on the CAP CwRS benchmarking standards.

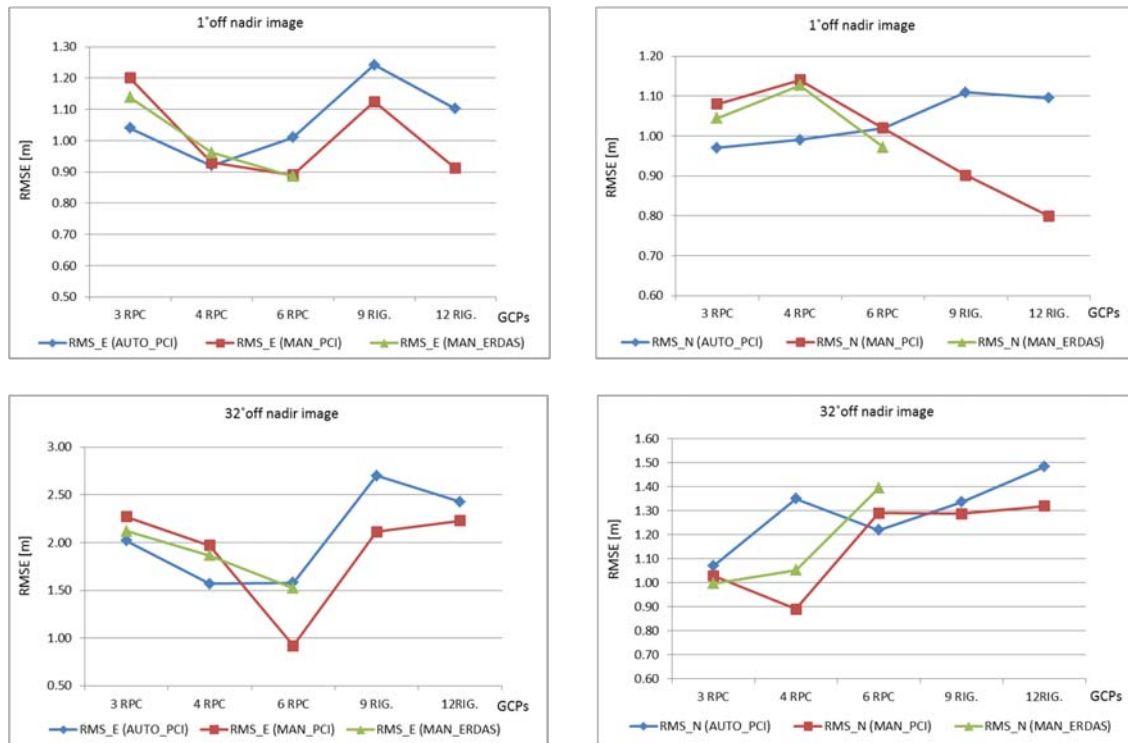


Figure 14: 1-D RMSE measured on the orthoimages as a function of the number of GCPs used for the modelling, with the focus on each GCPs detection methodology (and software)
 From up to down - from left to right: 1° off nadir angle scene - RMSEs in the Easting and Northing direction, 32° off nadir angle scene - RMSEs in the Easting and Northing direction.

On the basis of the comparison of the presented results, the following findings can be drawn:

- When 1° off nadir angle scene and RPC method is used for ortho production the measured RMSEs are very similar to each other and comparable for both methodologies. The differences vary within 16 cm. The alternative method gives slightly better results in this case.
- When 32° off nadir angle scene and RPC method is used for ortho production the differences between measured RMSEs are bigger and vary within 70cm. However the results are inconclusive.
- Further testing of the orthoimages processed with the RPC model and more than 6 GCPs would be necessary to follow the RMSEs progression.

- The standard manual benchmarking methodology provides better results (max dif. value is around 60cm) compare to alternative method for the rigorous model-based ortho imagery. The influence of the used methodology on the rigorous modelling results could be assessed only for PCI Geomatics 2013 since in ERDAS Imagine 2013 the rigorous model was not implemented.

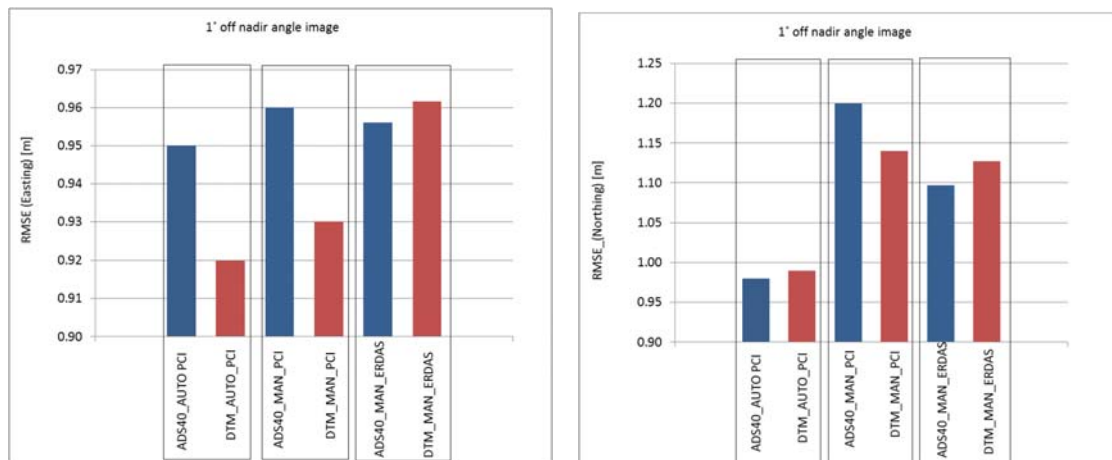
4. Discussion about DEM ADS40 and INTERMAP5m DTM

As correctly pointed out by the FW Contractor the DEM provided by JRC and usually used for the benchmarking purposes is in fact a digital surface model (DSM) roughly filtered to DTM for agriculture areas, see details in chapter 3.2 (benchmarking report). In case of DSM the orthorectification process calculates with altimetric values of objects on the ground (treetops..) instead of the correct ground altimetric values. As a consequence some noise and smearing effects may occur, especially for high off nadir angle acquisitions. For that reason the FW Contractor expressed the preference to use the INTERMAP 5 DTM (also provided by JRC).

Although it was agreed to use INTERMAP 5m DTM for the Kompsat-3 benchmarking purposes a test on a sample of images was performed to assure that the quality of the produced orthoimages is not degrade by applying of the nonstandard DEM.

The testing sample (i.e. both DEMs were used) of orthoimages was produced using two scenes (1° and 32° off nadir angle) both software (PCI, ERDAS) applying the RPC model, 4 GCPs and both the automatic and the manual selection of GCPs. In total 12 images were tested for this purpose.

4.1 Comparison between DEM ADS40 and INTERMAP 5m DTM and their potential influence on the final geometric accuracy of the orthoimage.



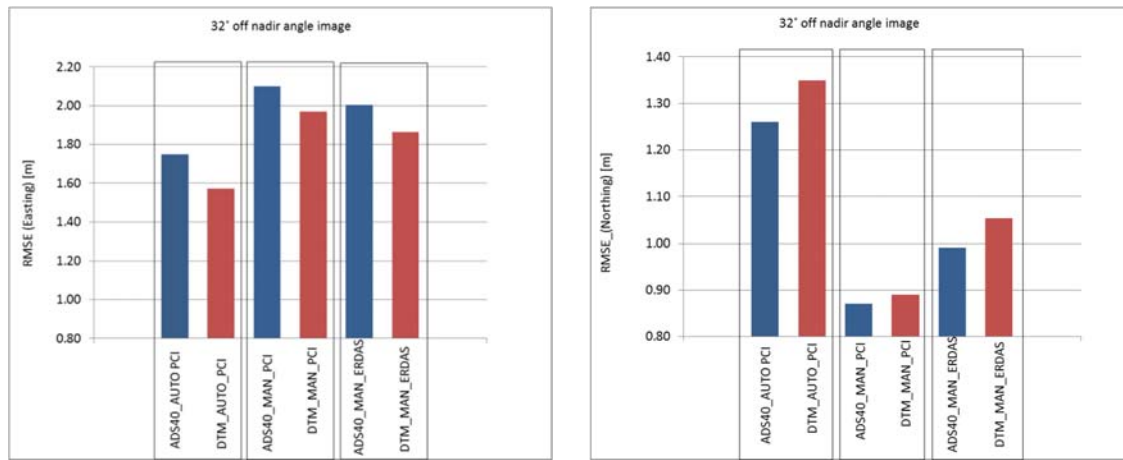


Figure15: 1-D RMSE comparison between the orthoimages processed with ADS40 and orthoimages processed with INTERMAP5mDTM

Graphs compare RMSEs measured on the orthoimages for which the same orthorectification procedure was used. From up to down, from left to right: 1° off nadir angle scene, RMSEs in the Easting direction and RMSEs in the Northing direction, 32° off nadir angle scene, RMSEs in the Easting direction and RMSEs in the Northing direction. For a simplicity the following abbreviations are used: DTM= INTERMAP5 DTM, MAN= manual selection of GCPs, AUTO= automatic selection of GCPs.

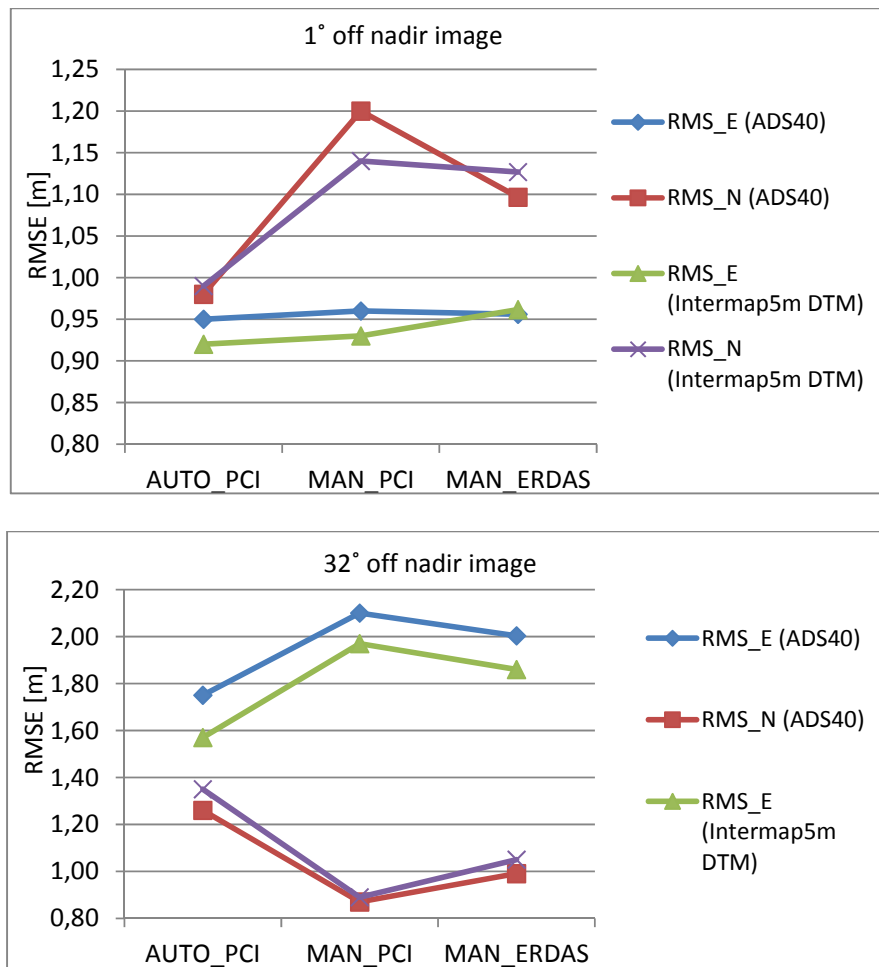


Figure16: 1-D RMSE measured on orthoimages as a function of methodologies used for ortho production.

Both figures, the Figure15 and the Figure16 express the same RMSE results. They differ from each other only in a way of displaying the RMSE values

Comparing the Kompsat-3 orthoimages produced using DEM ADS 40 and INTERMAP 5m DTM present the following findings:

- Regarding the DEM used for the ortho production no clear dependency of the RMSE values on the software or method of GCPs selection has been found
- RMSE values are very similar to each other. Maximum RMSE differences are 9cm for the Northing direction and 18 cm for the Easting direction.
- For the testing AOI both DEMs provide equal results as far as the horizontal accuracy is concerned.

4.2 Visual quality comparison of orthoimages produced using DEM ADS40 and INTERMAP 5 DTM

Although the geometric quality testing of the orthoimages led to the similar RMSE results, comparing the visual quality of images we can confirm less smearing effects when INTERMAP5mDTM was applied, especially in wooden areas. However looking at some steep slopes, also for INTERMAP5mDTM strong deformations appear (bottom-right image).

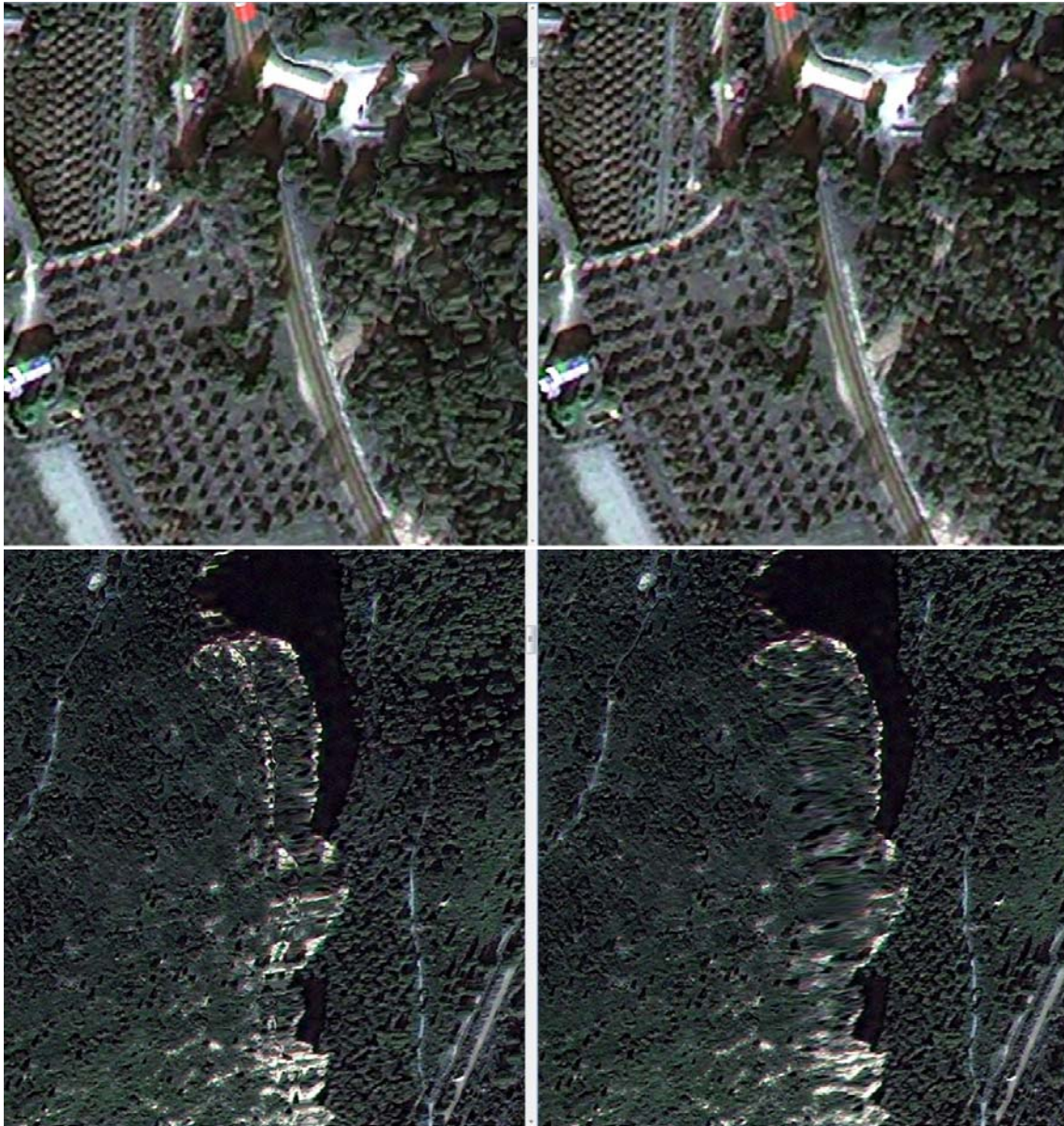


Figure17: Visual quality comparison between DEM ADS40 and INTERMAP5mDTM usage
Top: deformations in wooden-agriculture area, left:ADS40, right: INTERMAP5mDTM. Bottom: deformations in a hilly area, left:ADS40, right: INTERMAP5mDTM

More details about both DEMs can be found in the chapter 3.2 Digital Elevation Model (benchmarking report)

5. Additional test of 12° off nadir angle scene

Additional geometric quality assessment of ortho products generated from the 12° off nadir angle scene (i.e. GSD = 75 cm) has been performed. Due to the requirements put on the VHR prime profile regarding the GSD of the imagery used for the CwRS purposes, the acquisition (off nadir) angle of the KOMPSAT-3 satellite will be for this profile limited to 0°-14°. It is therefore needed to test the various factors (number of GCPs, models etc.) and set instructions which should be followed in order to produce the ortho product that complies with the VHR profile-based specifications. The special attention is given to the behaviour of RMSE when the rigorous model is used during the bundle adjustment since the results obtained from the 32° ONA ortho products do not comply with the VHR profile requirements.

PCI Geomatics 2013 (alternative weighting parameters)			RPC			Rigorous		DEM
			PCI		Erdas	PCI		
			manual [m]	auto [m]	manual [m]	manual [m]	auto [m]	
12°	0	East	35.99	n/a	35.80	n/a	n/a	INTERMAP _{5m} DTM
		North	9.95	n/a	10.16	n/a	n/a	
	3	East	1.53	n/a	1.42	n/a	n/a	
		North	0.78	n/a	0.78	n/a	n/a	
	4	East	1.53	n/a	1.38	n/a	n/a	
		North	0.76	n/a	0.69	n/a	n/a	
	6	East	n/a	n/a	n/a	2.64	n/a	
		North	n/a	n/a	n/a	0.85	n/a	
	9	East	n/a	n/a	n/a	2.11	n/a	
		North	n/a	n/a	n/a	0.74	n/a	
	12	East	n/a	n/a	n/a	1.99	n/a	
		North	n/a	n/a	n/a	0.80	n/a	

Table 5: Results of RMSE_{1D} measurements in JRC ICPs dataset.

The results are presented for the 12° viewing angle. The highest and lowest errors measured (per row) are marked with red and blue colours respectively. The values highlighted with the red font exceed the set value for the VHR prime profile (RMSE of 2m).

ANNEX I - External quality control of Kompsat-3 orthoimagery

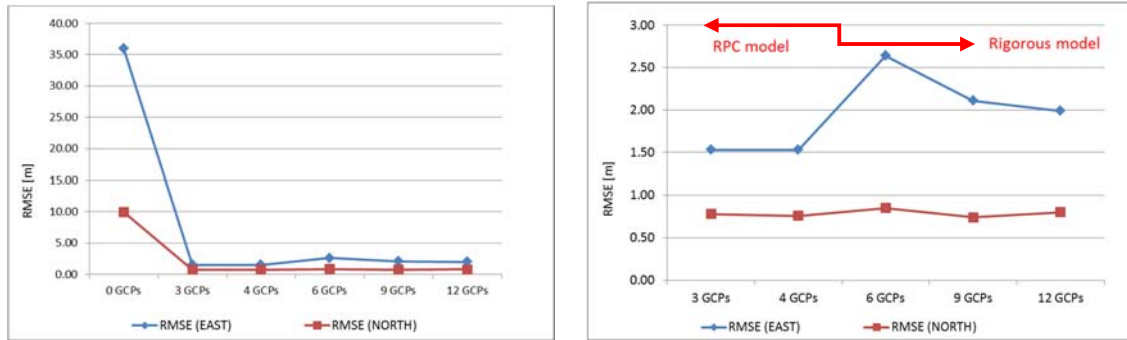


Figure18: 1-D RMSE measured on the orthoimages as a function of the number of GCPs used for the modelling.

Charts represent results using PCI software, RPC modelling with 3 and 4 GCPs, rigorous modelling with 6, 9, 12 GCPs. The chart on left contains 0 GCP variant, the right chart displays the same results excluding 0 GCP option (for better illustration)

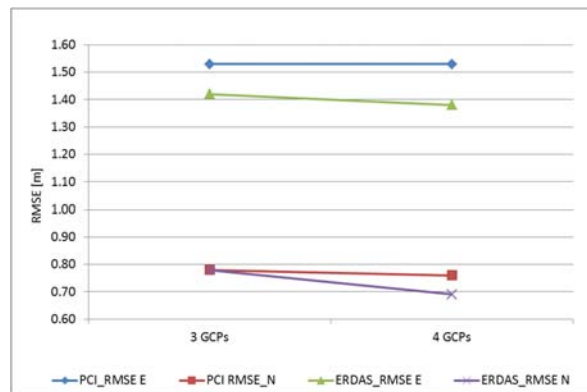


Figure 19: Comparison of RMSEs for 3 and 4 GCPs (RPC), using PCI and ERDAS software

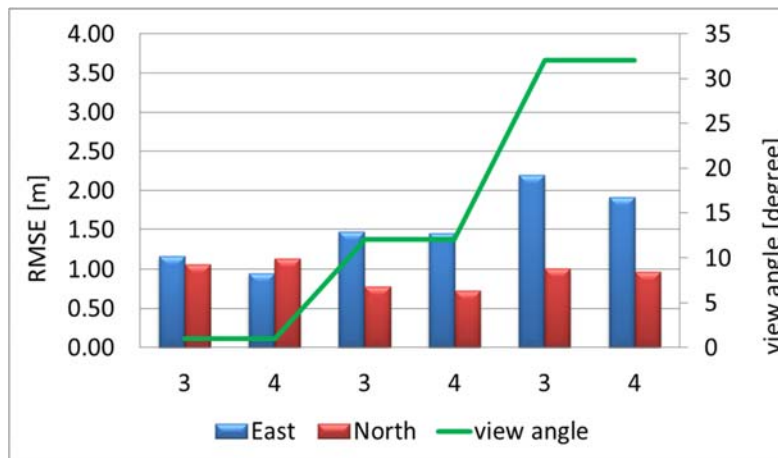


Figure 20: Graph of RMSEs as a function of the number of GCPs and off nadir angle - RPC model

The comparison is done for the orthoimages derived with INTERMAP5mDTM, the manual method of GCPs selection, RPC model

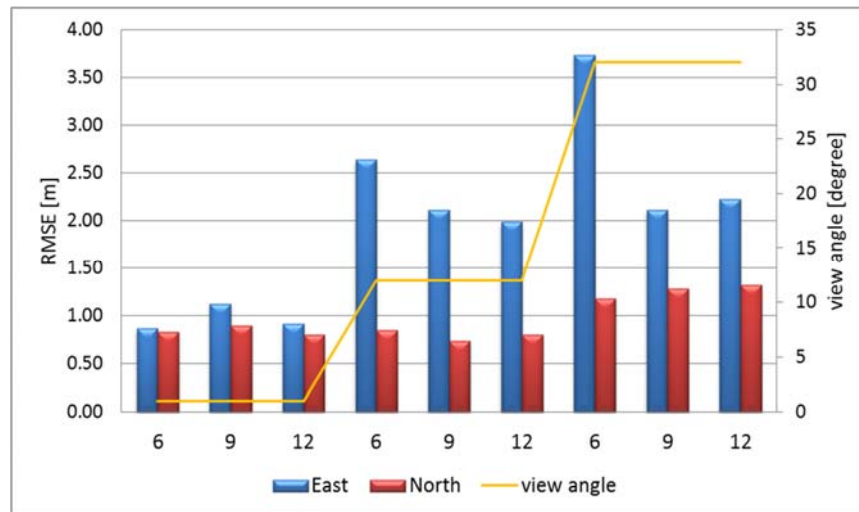


Figure 21: Graph of RMSEs as a function of the number of GCPs and off nadir angle

The comparison is done for the orthoimages derived with INTERMAP5mDTM, the manual method of GCPs selection, rigorous model

The Figure 21 displays the RMSEs behaviour as a function of all tested off nadir angles, when a rigorous modelling applied.

Looking at above mentioned results we've got by testing 12° off nadir angle scene we can summarise the following findings:

- The measured RMSEs meet the geometric specification of 2.0 m when RPC-based model is applied and at least 3 GCPs used for the modelling phase.
- Applying the rigorous model at least 12 well-distributed GCPs should be used to comply with the geometric criteria of 2.0 m.
- The values go along with already obtained results (1 °and 32 °off nadir angle images) and confirm the findings and conclusions summarised in previous chapters.

6. Conclusions

First of all, as regards the validation of the Kompsat-3 ortho products, on the basis of the presented results, some general conclusions can be drawn:

- The Kompsat-3 ortho imagery geometric accuracy meets the requirement of 5 m 1D RMSE corresponding to the VHR backup profile defined in the VHR profile based technical specifications.
- The Kompsat-3 ortho imagery geometric accuracy meets the requirement of 2 m 1D RMSE corresponding to the VHR prime profile defined in the VHR profile based technical specifications, on condition that RPC model and more than 4 GCPs are used to derive the ortho product. Note that the other requirement $GSD \leq 0.75m$ set up for the VHR prime profile restricts the off nadir acquisition angle to 13° - 14° . Following this restriction already using 3GCPs gives required results.
- The Kompsat-3 ortho imagery geometric accuracy does not meet the requirement of 2 m 1D RMSE corresponding to the VHR prime profile defined in the VHR profile based technical specifications when a high off nadir angle image (in our case 32° off nadir) in a combination with the rigorous model are used for the ortho production. Having 12° off nadir angle image 12 GCPs should be used to meet the requirement of 2 m.

Secondly, as regards the factors influencing the final ortho image accuracy, some general conclusions can be drawn:

- The geometric accuracy of Kompsat-3 ortho imagery displays a significant dependence on the off nadir angle, especially in the Easting direction (higher accuracy for lower off nadir angle). See the chapters 2.2 and 5.
- Overall the accuracy is practically software independent. Both software tested provide very similar results and suit for the ortho image generation with the accuracy required by CwRS technical specifications. See the chapter 2.3.
- Using both models, the Rational Polynomial Function model and Tutin's Rigorous model give similar RMS errors for the close off nadir image. See the chapter 2.4.
- Applying the rigorous model on high off nadir angle image results in a worse accuracy of the East component (3-4m). See the chapter 2.4.
- No clear correlation between the measured RMSEs and the number of GCPs has been found. See the chapters 2.5 and 5.

Lastly, as regards the additional assessment of the alternative benchmarking methodology and DEM usage, the following conclusions can be drawn:

- Applying the Rational Polynomial Functions model and a reasonable number of ground control points (i.e 3 and more) the proposed alternative benchmarking methodology performs equally to the standard one. See the chapter 3.
- The standard manual benchmarking methodology keeps better results for the Tutin's Rigorous model- based ortho imagery. See the chapter 3.
- As far as the influence of DEM on the final ortho product geometric accuracy is concern, applying both of them resulted in the orthoimages of the same geometric quality. However, it is necessary to mention that the majority of the ICPs for which the residuals were measured are situated in the flat agricultural area thus where the smearing effects, in our case, do not appear. See the chapter 4.

7. Additional comments

JRC has received via EUSI a confirmation note regarding the Kompsat-3 Image quality (Sensor alignment calibration) made out by SI Imaging Service ('worldwide exclusive representative' for Kompsat imagery sales). The document confirms that the Kompsat-3 processing software was updated and therefore the data processed after 14.11.2014 (ie image acquisition campaign 2015 onwards) are East direction error free.

Due to this adjustment all tested software ERDAS 2013, PCI Geomatics 2013 (and their updates) should provide correct unbiased results.

All EQO reports are archived in:

<\\ies.jrc.it\Ho4\Common\Data\CID\MAUSSANE\KOMPSAT-3\FINAL REPORTING\ANNEX III>

Europe Direct is a service to help you find answers to your questions about the European Union
Freephone number (*): 00 800 6 7 8 9 10 11

(*): Certain mobile telephone operators do not allow access to 00 800 numbers or these calls may be billed.

A great deal of additional information on the European Union is available on the Internet.
It can be accessed through the Europa server <http://europa.eu>.

How to obtain EU publications

Our publications are available from EU Bookshop (<http://bookshop.europa.eu>),
where you can place an order with the sales agent of your choice.

The Publications Office has a worldwide network of sales agents.
You can obtain their contact details by sending a fax to (352) 29 29-42758.

European Commission
EUR 27064 – Joint Research Centre – Institute for Environment and Sustainability

Title: New sensors benchmark report on Kompsat-3

Author(s): Blanka Vajsova, Agnieszka Walczynska, Samuel Bärtsch, Pär Johan Åstrand, Susanne Hain

Luxembourg: Publications Office of the European Union

2015 – 58 pp. – 21.0 x 29.7 cm

EUR – Scientific and Technical Research series – ISSN 1831-9424

ISBN 978-92-79-45054-9

doi:10.2788/240349

JRC Mission

As the Commission's in-house science service, the Joint Research Centre's mission is to provide EU policies with independent, evidence-based scientific and technical support throughout the whole policy cycle.

Working in close cooperation with policy Directorates-General, the JRC addresses key societal challenges while stimulating innovation through developing new methods, tools and standards, and sharing its know-how with the Member States, the scientific community and international partners.

*Serving society
Stimulating innovation
Supporting legislation*

doi:10.2788/240349

ISBN 978-92-79-45054-9

